Synthesis, Characterization, and Enhanced Photocatalytic Degradation of PFAS in Water Using Cu_2S Nanostructures

Maryam Tabatabaei

A Thesis in the Department

Of

Building, Civil and Environmental Engineering (BCEE)

Presented in Partial Fulfillment of the Requirements

For the Degree of

Master of Applied Science (Environmental Engineering)

At Concordia University

Montreal, Quebec, Canada

December 2025

CONCORDIA UNIVERSITY

School of Graduate Studies

This is to certify that the thesis prepared

By: Maryam Tabatabaei

Entitled: Synthesis, Characterization, and Enhanced Photocatalytic Degradation of PFAS in Water Using Cu_2S Nanostructures

and submitted in partial fulfillment of the requirements for the degree of

Master of Applied Science (Environmental Engineering)

complies with the regulations of this University and meets the accepted standards with respect to

originality and quality.

Signed by the Final Examining Committee:

_____Chair
Dr. Catherine Mulligan

_____Examiner
Dr. Chunjiang An

_____Examiner
Dr. Catherine Mulligan

_____Supervisor
Dr. Jae-Hoon Hwang

Abstract

Synthesis, Characterization, and Enhanced Photocatalytic Degradation of PFAS in Water Using Cu_2S Nanostructures

Maryam Tabatabaei

Per- and polyfluoroalkyl substances (PFAS), including perfluorooctanoic acid (PFOA) and perfluorooctanesulfonic acid (PFOS), are persistent environmental pollutants widely detected in water due to their extensive industrial and urban applications. Their bioaccumulative and toxic nature is associated with adverse health effects, including thyroid dysfunction, hepatotoxicity, immune suppression, and potential carcinogenicity, as well as ecological impacts such as microbial community disruption and the propagation of antibiotic resistance genes. Conventional PFAS removal methods, including adsorption, ion exchange, and membrane processes, are constrained by high costs, the generation of secondary waste, and limited efficiency for short-chain PFAS.

Photocatalysis, an advanced oxidation process, presents a sustainable approach for the complete defluorination and mineralization of PFAS under mild conditions. However, traditional photocatalysts such as TiO_2 are restricted by their wide band gap and UV light dependence, prompting the exploration of alternative materials. While gallium oxide, indium oxide, and graphitic carbon nitride have been investigated, their photocatalytic performance remains constrained by limited solar absorption and rapid charge carrier recombination.

This study focuses on the synthesis, characterization, and enhanced photocatalytic degradation of Cu_2S nanostructures for the removal of PFOA and PFOS in water. The materials, including CuS, Cu_2S, a mixed-phase (Cu_2S/CuS) $Cu_2S3/2$, and Cu_2S

integrated with reduced graphene oxide (rGO), were synthesized via hydrothermal and solvothermal methods, thoroughly characterized, and tested under UV irradiation to assess their degradation efficiency and potential synergistic effects in composite systems. Among the prepared photocatalysts, $Cu_2S3/2$ exhibited the highest degradation activity, achieving up to 99% PFOS removal and 93% PFOA degradation, while Cu_2S showed comparable efficiency. In contrast, the Cu_2S/rGO composite displayed moderate degradation efficiency of 76%.

These results highlight the potential of Cu-based nanostructures, whose tunable morphologies and favorable photoactive properties offer promising solutions to current limitations in PFAS treatment. The observed high degradation efficiencies, combined with the versatility of the synthesis methods, suggest that these Cu_2S nanostructures can be further optimized for large-scale water remediation applications. Overall, this work demonstrates the enhanced photocatalytic performance of Cu_2S nanostructures in water remediation, providing a comprehensive framework for the design of effective, scalable, and environmentally sustainable strategies to manage emerging contaminants such as PFAS. These findings not only advance the understanding of copper sulfide–based photocatalysts but also offer practical insights for addressing persistent water pollutants in real-world scenarios.

Keywords: Advanced catalysts, PFAS photocatalysis, Copper sulfide photocatalyst materials, PFAS degradation, Visible-light photocatalyst, Water treatment

Acknowledgments

It is with great pleasure that I extend my sincere appreciation to Concordia University for granting me the opportunity to pursue my master's degree in such an inspiring academic environment. I am truly grateful for the support and resources that made this journey possible.

My deepest gratitude goes to my supervisor, Dr. Jae-Hoon Hwang, whose exceptional guidance, encouragement, and dedication have shaped every step of this project. His unwavering support and expertise were instrumental to the completion of this work, and I am sincerely thankful for his inspiring leadership.

I also wish to express my heartfelt thanks to my parents, whose lifelong love and encouragement have been the foundation of all my achievements. Even from afar, their support has remained a constant source of strength and comfort, making every challenge along this journey meaningful and worthwhile.

Table of Contents

List of Figures

List of Tables

Chapter 1: Introduction

1.1 PFAS Material Properties and Effects

Per- and polyfluoroalkyl substances (PFAS), such as perfluorooctanoic acid (PFOA) and perfluorooctanesulfonic acid (PFOS), have become widespread environmental pollutants due to their extensive use in industrial and urban activities (Aditi, 2021; Kotthoff et al., 2015; Zareitalabad et al., 2013). High levels of PFAS are often found near airports, textile facilities, and metal industries, where they threaten drinking water safety. Long-chain PFAS enter aquatic systems through industrial discharge and atmospheric deposition, creating serious environmental and health concerns (Aditi, 2021; Tabatabaei et al., 2025; Zhang et al., 2016b). PFAS are highly persistent, bioaccumulative, and toxic compounds linked to various health risks, including thyroid dysfunction, liver damage, immune suppression, reproductive toxicity, and potential carcinogenicity. They disrupt endocrine function by interfering with thyroid hormone activity and contribute to hepatotoxicity through altered lipid metabolism and enzyme regulation (Grandjean and Clapp, 2015; Post et al., 2012; Sadia et al., 2023; Tabatabaei et al., 2025).

Additionally, PFAS accumulation in aquatic environments disrupts microbial community structures (Liu and Mejia Avendaño, 2013) and facilitates the spread of antibiotic resistance genes (ARGs), as observed in several PFAS-contaminated environments (Liu et al., 2023; Yashir et al., 2025). These impacts underscore the urgent need for global regulatory frameworks capable of addressing not only long-chain but also ultra-short-chain PFAS, which are often inadequately managed (Neuwald et al., 2022; Zhang et al., 2016b). Sources of PFAS contamination, such as aqueous film-forming foams, non-stick coatings, and industrial runoff, continue to threaten both drinking water quality and aquatic ecosystems (Podder et al., 2021), necessitating strong

international cooperation and standardized mitigation strategies. For example, the U.S. Environmental Protection Agency (USEPA, 2024) has set stringent limits for PFOA and PFOS in drinking water at 0.0040 ppb to reduce health risks (USEPA, 2024).

1.2 PFASs Treatment Methods

A wide range of treatment technologies has been developed to remove PFAS from water, including physical adsorption methods using granular activated carbon (GAC), powdered activated carbon (PAC), ion exchange resins, molecularly imprinted polymers (MIPs), and bio-based materials (Leung et al., 2022; Wanninayake, 2021a; Zhang et al., 2016a). However, these approaches face critical limitations in terms of cost, efficiency, especially against short-chain PFAS, and secondary waste generation (Ateia et al., 2019; McCleaf et al., 2017). Similarly, membrane-based processes like nanofiltration (NF) and reverse osmosis (RO) demonstrate effective PFAS removal, but are hindered by operational complexity, energy intensity, fouling issues, and high capital costs (Mastropietro et al., 2021). Consequently, there is growing interest in developing more sustainable and efficient PFAS treatment technologies.

In recent years, catalytic degradation methods, particularly photocatalysis, have emerged as promising alternatives due to their potential to achieve complete defluorination and mineralization of PFAS under relatively mild conditions (Olatunde et al., 2020; Trojanowicz et al., 2018). Photocatalysis, a type of advanced oxidation process (AOP), has demonstrated superior degradation efficiency and versatility compared to conventional methods such as adsorption and ozonation (Chen et al., 2023; Luo et al., 2024b; Xu et al., 2017). Other AOPs, including electrochemical oxidation, sonolysis, plasma treatment, photo-Fenton reactions, and radiolysis, have also shown promising PFAS degradation performance (Verma et al., 2024; Wang et al., 2014;

Xin et al., 2023). Despite these advancements, commonly used photocatalysts like titanium dioxide (TiO_2) remain limited by their wide band gap and reliance on ultraviolet (UV) light, which constitutes only a small fraction of the solar spectrum. Alternatives such as gallium oxide, indium oxide, and graphitic carbon nitride have also been studied, yet suffer from low solar utilization and fast recombination of photogenerated charges, which inhibits reactive species formation and degrades photocatalytic efficiency.

To address these shortcomings, current research is focused on designing nanostructured, visible-light-responsive photocatalysts that can utilize a broader range of the solar spectrum and facilitate efficient charge separation. Nanostructuring the photocatalyst material further enhances photocatalytic activity by increasing surface area, light absorption, and charge carrier mobility. In this context, copper (I) sulfide (Cu_2S) has attracted growing interest for its strong visible to near-infrared (NIR) photoactivity, favorable band gap, and high potential for forming heterojunctions that improve charge separation. Cu_2S-based materials have already demonstrated effectiveness in the degradation of various organic pollutants, such as methylene blue and tetracycline, highlighting their potential in wastewater treatment applications. Their photoactive nature, tunable electronic properties, and morphological flexibility make them suitable candidates for PFAS degradation under solar or simulated solar irradiation (Ait-Karra et al., 2023; Xu et al., 2015).

1.3 Research Objective

This research focuses on the synthesis, characterization, and evaluation of copper-based photocatalysts, CuS, Cu_2S, a mixed-phase $Cu_2S_{3/2}$, and Cu_2S supported on reduced graphene oxide (rGO), with the primary purpose of assessing their applicability for PFAS (PFOA and PFOS) degradation in water. Cu_2S nanoparticles were synthesized via a hydrothermal process at 180 °C,

while CuS and Cu_2S/CuS were prepared using solvothermal synthesis at 120 °C. The resulting materials were characterized by scanning electron microscopy (SEM) and X-ray diffraction (XRD). Photocatalytic activity was tested in a sealed UV reactor (245–365 nm, 6 W) under room temperature and mildly acidic conditions (pH 4–5), employing 20 mg of catalyst for 8 hours with continuous stirring. PFAS degradation was quantified using liquid chromatography–mass spectrometry (LC-MS). Among the tested photocatalysts, $Cu_2S3/2$ demonstrated the highest activity, achieving up to 99% removal of PFOS and 93% of PFOA, followed by Cu_2S, while the Cu_2S/rGO composite exhibited moderate efficiency, reaching 76% degradation. By addressing limitations in current treatment technologies and advancing copper-based nanomaterials, this study contributes to the development of scalable and environmentally sustainable solutions for PFAS remediation in water.

Chapter 2: Background and Literature Review

2.1 PFASs Remediation Technologies and Challenges

PFASs including PFOA and PFOS, are highly persistent, bioaccumulative, and toxic environmental contaminants that pose serious threats to aquatic ecosystems, drinking water quality, and human health. Exposure to PFAS has been associated with numerous adverse effects, including thyroid dysfunction, liver damage, immune suppression, reproductive toxicity, and potential carcinogenicity. Conventional treatment technologies, such as adsorption, membrane filtration, and ozonation, can reduce PFAS concentrations but are often limited by high operational costs, energy-intensive processes, and the generation of secondary waste (Tabatabaei et al., 2025). In response to these challenges, advanced oxidation processes (AOPs) have been developed to degrade PFAS through the formation of highly reactive species. Techniques such as electrochemical oxidation, sonolysis, plasma treatment, photo-Fenton reactions, and radiolysis have demonstrated promising degradation efficiencies. Among AOPs, photocatalysis has emerged as a particularly effective method due to its ability to harness light energy to drive chemical reactions under relatively mild conditions.

2.2 Photodegradation Method and Materials

Photocatalysis is initiated when a semiconductor absorbs light in the ultraviolet (UV) or visible spectrum, exciting electrons from the valence band to the conduction band and generating electron–hole pairs. These charge carriers react with water and oxygen to form reactive oxygen species (ROS), including hydroxyl radicals (•OH) and superoxide anions ($\bullet O_2^-$), which degrade

PFAS molecules. The degradation proceeds via partial photo-oxidation, breaking pollutants into smaller, less harmful compounds, or complete mineralization into carbon dioxide (CO_2) and fluoride ions (F^-). Photocatalysts also enhance efficiency by adsorbing pollutants on their surfaces, concentrating them for more effective degradation. Environmental factors such as pH, temperature, and the presence of natural organic matter can influence photocatalytic performance by affecting light absorption and ROS availability, while understanding the formation of intermediates is critical for optimizing efficiency and ensuring safe byproducts (Tabatabaei et al., 2025). A wide range of semiconductors have been explored for PFAS degradation, including titanium dioxide (TiO_2), gallium (III) oxide (Ga_2O_3), indium(III) oxide (In_2O_3), zinc oxide (ZnO), cadmium sulfide (CdS), tungsten trioxide (WO_3), graphitic carbon nitride (g-C_3N_4), bismuth oxychloride (BiOCl), and tungstic heteropolyacid ($H_3PW_{12}O_{40}$). Despite these advances, many materials face limitations such as wide band gaps restricting light absorption, fast recombination of photogenerated electrons and holes, and low utilization of solar energy. Strategies including metal/non-metal doping, formation of heterojunctions, co-catalyst integration, and incorporation of carbon-based materials have been employed to improve charge separation, enhance ROS generation, and boost overall photocatalytic efficiency (Tabatabaei et al., 2025).

2.3 Cu_2S Based Photocatalyst

Among emerging materials, copper(I) sulfide (Cu_2S) nanomaterials have gained significant attention due to their strong photoactivity and versatility, making them promising candidates for photocatalysis, hydrogen production, and photothermal therapy. Cu_2S exhibits a suitable band gap for visible and near-infrared (NIR) light absorption, enabling efficient utilization of solar energy. The formation of heterojunctions with other semiconductors, such as CdS, $ZnIn_2S_4$, and MoS_2,

enhances the separation and transfer of photogenerated electrons and holes, reduces charge recombination, and improves photocatalytic efficiency (Hwang et al., 2021; Liu et al., 2018; Roy and Srivastava, 2015). In pollutant degradation, nanoporous and hydrothermally synthesized CuS, which can form from Cu_2S, has been shown to efficiently degrade dyes like methylene blue and tetracycline, demonstrating strong potential for wastewater treatment (Ain et al., 2022). Additionally, Cu_2S-based heterostructures, such as $Cu_{2-x}S/CdS/Bi_2S_3$ and MoS_2-stratified CdS-$Cu_{2-x}S$, exhibit high hydrogen evolution rates under visible and NIR light due to enhanced charge separation and surface area. Cu_2S nanomaterials also display strong NIR absorption and high photothermal conversion efficiency, making them suitable for photothermal therapy and imaging when combined with other materials such as gold or as ultrasmall nanodots (Nikam et al., 2020; Wang et al., 2015). Despite these promising properties, there are several gaps in the current studies regarding Cu_2S photocatalysts for PFAS degradation. Studies specifically investigating PFAS removal using Cu_2S remain limited, and there is a lack of long-term stability tests to evaluate the durability and reusability of these photocatalysts. Furthermore, the mechanistic pathways underlying PFAS degradation by Cu_2S are not yet fully understood, including the identification of intermediates and the roles of reactive oxygen species in defluorination and mineralization processes.

This thesis aims to address these gaps by investigating the application of Cu_2S photocatalysts for PFAS removal from aqueous systems, focusing on optimizing reaction conditions, elucidating degradation mechanisms, and evaluating photocatalytic efficiency. By leveraging the unique electronic structure, tunable morphology, and heterojunction-forming capabilities of Cu_2S, this research seeks to advance the development of efficient and practical photocatalytic strategies for the treatment of PFAS-contaminated water.

Chapter 3: Photocatalytic innovations in PFAS removal: Emerging trends and advances (Adapted from a Published Review Article)

This chapter is adapted from a peer-reviewed review article published by the candidate as first author: Photocatalytic innovations in PFAS removal: Emerging trends and advances, Science of The Total Environment 980, 179567.

The content has been reformatted and partially revised to comply with thesis guidelines.

3.1 Introduction and Scope of the Review

PFAS, such as PFOA and PFOS, have become widespread environmental pollutants due to their extensive use in industrial and urban activities (Aditi et al., 2021; Kotthoff et al., 2015; Zareitalabad et al., 2013). High concentrations of PFAS are frequently detected in areas near airports, textile mills, and metal smelting industries, where they compromise the safety of drinking water sources. Long-chain PFAS are introduced into aquatic systems through industrial effluents and atmospheric deposition, posing significant environmental and health challenges (Aditi et al., 2021; Brown et al., 2020; Zhang et al., 2016b). Despite regulatory efforts, many frameworks inadequately address ultra-short-chain PFAS, emphasizing the critical need for a globally unified regulatory approach. Current regulations often fail to manage PFAS comprehensively, especially ultra-short-chain variants, highlighting the necessity for more inclusive global regulatory strategies (Neuwald et al., 2022; Zhang et al., 2016b).

PFAS contamination stems from multiple sources, including aqueous film-forming foams, non-stick coatings, and industrial runoff, all of which have a negative impact on marine ecosystems and drinking water supplies. Exposure to these substances has been linked to various adverse health effects such as thyroid dysfunction, liver damage, immune suppression, reproductive issues, and potential carcinogenic risks. To effectively address these concerns, strong international collaboration and standardized mitigation strategies are essential to protect both public health and the environment. In response, current regulations, such as the National Primary Drinking Water Regulations (NPDWR), set an extremely low permissible limit of 0.0040 parts per billion (ppb) for PFOA and PFOS in drinking water (USEPA, 2024).

Various treatment technologies have been developed to remove PFAS from water. Among these, physical adsorption methods, including granular activated carbon (GAC), powdered activated

carbon (PAC), anion exchange (AIX), molecularly imprinted polymers (MIP), and biomaterials, have been widely investigated for their removal efficiency (Leung et al., 2022; Wanninayake, 2021a; Zhang et al., 2016a). In addition, high-pressure-driven membrane processes, such as nanofiltration (NF) and reverse osmosis (RO), have demonstrated substantial effectiveness in separating PFAS (Leung et al., 2022; Wanninayake, 2021a). However, each method has inherent limitations. Adsorption is valued for its high capacity and operational simplicity, but frequent replacement or regeneration, secondary waste generation, and substantial energy demands result in high operational costs. Similarly, ion-exchange resins effectively capture PFAS but require chemically intensive regeneration processes, increasing costs and complicating waste management.

Their efficiency decreases when targeting short-chain PFAS due to their higher mobility. Reverse osmosis, while capable of removing a wide range of contaminants, is constrained by high energy demands, intensive membrane maintenance, and brine waste disposal challenges, making it a costly long-term solution (Ahmed et al., 2020; Verma et al., 2024; Wanninayake, 2021b; Xu et al., 2021). While traditional PFAS removal techniques like GAC, PAC, and RO offer some effectiveness, their high costs and maintenance challenges make them less practical for long-term applications. To address these challenges, catalytic technologies have emerged as innovative and promising alternatives.

Photocatalytic methods have attracted considerable attention for PFAS degradation and defluorination, due to their potential to address various environmental and energy-related challenges (Olatunde et al., 2020). Recent advancements have demonstrated promising outcomes, achieving complete PFAS mineralization through biological degradation and advanced oxidation processes (AOPs), including photochemical, sonolysis, electrochemical, thermolysis, chemical oxidation and reduction, plasma, subcritical, and radiochemical treatments (Trojanowicz et al.,

2018; Zhang et al., 2022). Among these, photochemical processes have shown remarkable PFAS dissociation and defluorination under ambient conditions, underscoring their potential as a key technology for PFAS degradation (Verma et al., 2024; Xin et al., 2023). Moreover, AOPs, such as electrochemical methods, radiation, ultrasound, ozonation, Fenton and photo-Fenton reactions, and plasma treatments, have emerged as effective alternatives to conventional approaches (Wang et al., 2014). Recent studies have highlighted photocatalysis as a highly promising approach for PFAS removal, offering advantage over conventional methods such as adsorption and ozonation in terms of pollutant degradation efficiency and versatility. This advanced technology demonstrates considerable potential for addressing persistent organic pollutants and achieving cleaner and safer environments (Bentuo Xu a b, 2017; Chen et al., 2023; Luo et al., 2024a).

This review summarizes a comprehensive overview of the latest advancements in photodegradation mechanisms and pathways of PFAS. Furthermore, it details recent advancements aimed at enhancing photocatalyst activity, addressing critical gaps in current research, and explores the mechanisms and structure-performance relationships between PFAS chemical structures and their removal efficiencies. The review highlights technological innovations and future directions for sustainable water treatment solutions.

3.2 Fundamental Principles of Photocatalytic PFAS Degradation

Photocatalysis, a light-driven process, enhances chemical reactions through the action of a catalyst and is particularly effective in degrading persistent pollutants such as PFAS (Deng et al., 2023). This process is initiated when a photocatalyst absorbs light, typically in the ultraviolet (UV) or visible spectrum, resulting in the excitation of electrons from valence band to the conduction band.

This excitation generates electron-hole pairs, which are crucial for initiating subsequent chemical reactions (Ahmed and Haider, 2018; Poulopoulos et al., 2019). These pairs react with water and oxygen form highly reactive species, such as hydroxyl radicals (•OH) and superoxide anions ($•O_2^-$), which drive the degradation of PFAS molecules.

The breakdown of PFAS proceeds via photo-oxidation, where pollutants are transformed into smaller, less harmful compounds, or mineralization, which fully decomposes them into carbon dioxide (CO_2) and fluoride ions (F^-) (Liu et al., 2020; Verma et al., 2021). The photocatalyst plays a critical role, not only in generating these reactive species but also in adsorbing pollutants onto its surface, thereby enhancing the degradation efficiency (Verma et al., 2024). Environmental conditions, including pH, temperature, and the presence of natural organic matter, can significantly affect photocatalytic efficiency by influencing UV light absorption and availability of reactive species.

Optimizing photocatalysis requires a comprehensive understanding of its underlying mechanisms, including the identification of intermediates formed during PFAS degradation, to improve process efficiency and ensure the safety of resulting byproducts (Bentuo Xu a b, 2017). Semiconductors, such as titanium dioxide (TiO_2), are commonly employed due to their ability to absorb light and generate charge carriers that facilitate pollutant degradation, including compounds like PFOA(Haghighi and Haghighat, 2024; Zhang et al., 2019a; Zhu et al., 2020).

In addition to TiO_2, alternative materials such as gallium(III) oxide (Ga_2O_3) and indium(III) oxide (In_2O_3) have shown promising results in PFAS degradation due to their superior photocatalytic properties in specific structural forms. The effectiveness of these semiconductors is largely determined by their bandgap, which governs their ability to absorb light within the UV-visible spectrum (Fu et al., 2022; Li et al., 2012). Other materials, including zinc oxide (ZnO),

cadmium sulfide (CdS), and tungsten trioxide (WO_3), are also explored for their distinctive electronic properties.

Recent innovations, such as incorporating carbon-based materials with conventional photocatalysts like TiO_2, have proven effective in reducing charge recombination, thereby enhancing photocatalytic performance (Nawaz et al., 2024). Emerging candidates like bismuth oxychloride (BiOCl) nanosheets and tungstic heteropolyacid ($H_3PW_{12}O_{40}$) exhibit significantly higher activity compared to traditional TiO_2, broadening the scope of photocatalytic materials for environmental remediation (Fig.3.1) (Huu-Tuan Do and Chao-Wei Huang, 2020; Luo et al., 2024a; Mills et al., 1993; Pelaez et al., 2012; Wu et al., 2022). Further advancements, including metal or non-metal doping, the creation of heterojunctions, and the integration of co-catalysts, improve charge separation and enhance the generation of reactive oxygen species. These developments aim to maximize the efficiency and applicability of photocatalysis for addressing PFAS and other recalcitrant pollutants (Ge et al., 2019; Khan et al., 2023; Luo et al., 2024a).

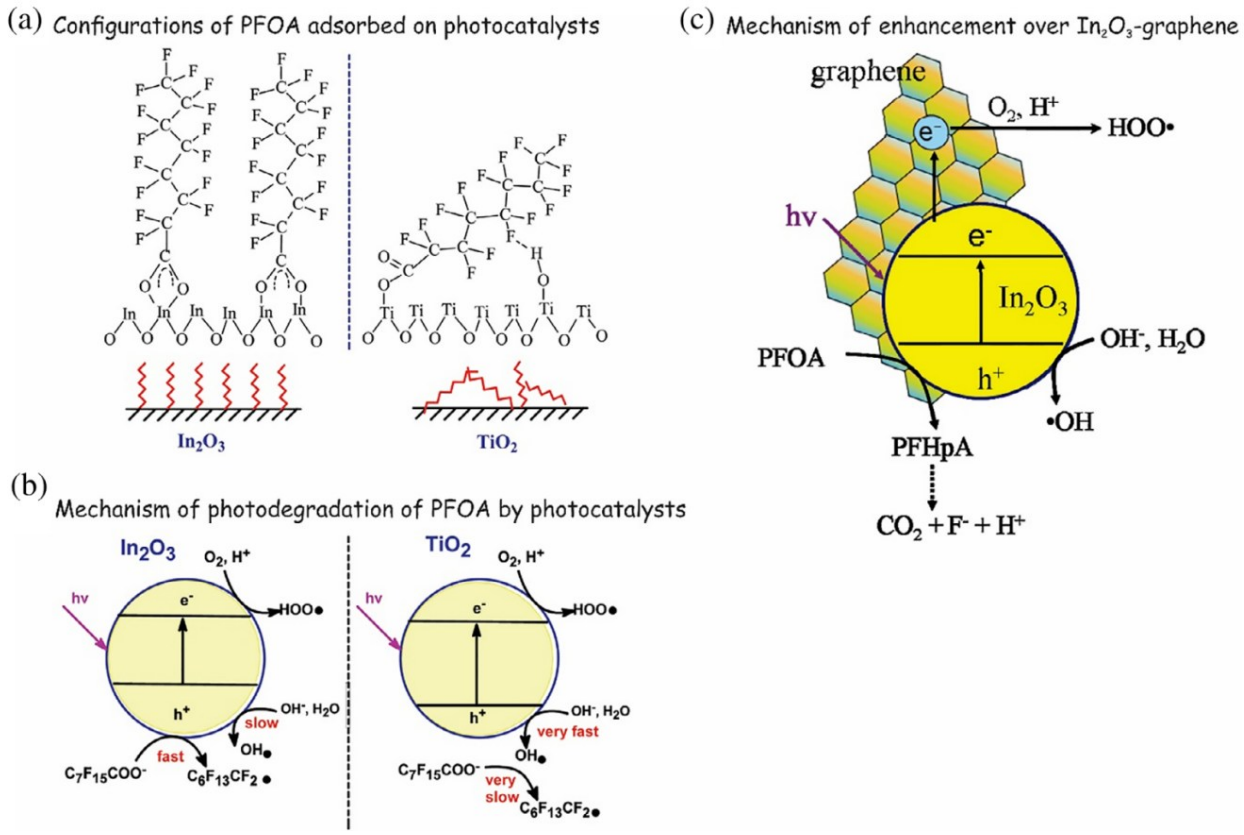

Figure 3.1 Comparison of (a) PFOA configurations adsorbed on indium (III) oxide (In_2O_3) and titanium dioxide (TiO_2), (b) mechanism of the photodegradation of PFOA by In_2O_3 and TiO_2, and (c) mechanism of photocatalytic activity enhancement over In_2O_3-graphene (Huu-Tuan Do and Chao-Wei Huang, 2020).

3.3 Photocatalytic Strategies for PFAS Removal

Recent advancements in photocatalytic PFAS degradation focus on enhancing efficiency and sustainability through both direct and indirect processes (Luo et al., 2024b). Direct photolysis breaks down PFAS molecules by having them directly absorb light, which causes their decomposition. In contrast, indirect photocatalysis uses reactive oxygen species (ROS), like hydroxyl radicals (•OH), superoxide anions (O_2•$^-$), and singlet oxygen (O_2), produced by a photocatalyst to degrade PFAS (Xin et al., 2023). Recent efforts focus on developing eco-friendly photocatalysts by replacing toxic and scarce heavy metals with environmentally benign materials,

such as Ti, Fe, In, Ga, Bi, Si, and BN, which maintain high performance (Juve et al., 2024). Innovations in photocatalyst synthesis aim to enhance visible light energy harvesting and photocatalytic efficiency. Advance designs, including nanostructured metal oxides and porous microspheres, increase surface area and optimize electronic properties. Integrating photocatalysis with advanced oxidation processes (AOPs) is gaining attention, as it promotes diverse ROS generation for improved PFAS degradation (Zango et al., 2023). Strategies such as defect engineering, oxygen vacancies, metal-doping, and heterojunction formation further enhance ROS production and catalytic activity.

The application of specific wavelengths, such as 185 nm for PFOA degradation, and the development of nano 3D structures to improve electron and mass transfer are critical for system optimization (Ren et al., 2022; Tang et al., 2023). Understanding the reaction mechanisms, including the identification of intermediates and radicals involved in PFAS photodissociation, is essential for refining photocatalytic systems and assessing their environmental impacts (Liang et al., 2023). Finally, performance validation across various water matrices is emphasized to evaluate cost-effectiveness, energy consumption, and life cycle impacts of these emerging technologies (Chen et al., 2023; Verma et al., 2024). Recent advancements in photocatalytic technologies have identified several promising photocatalysts for the effective degradation of PFAS.

3.3.1 Photochemical Oxidants

Photochemical oxidants are essential in enhancing the efficiency of photocatalysis, particularly in the degradation of persistent organic pollutants like PFAS. Activated by UV light, oxidants such as persulfate and hydrogen peroxide generate highly reactive radicals, including hydroxyl (•OH) and sulfate ($SO_4^{\bullet -}$) radicals. These radicals are highly effective in breaking down

complex PFAS molecules into simpler, less harmful compounds, significantly increasing the mineralization rates. In addition to accelerating reaction kinetics, the present of oxidants improves the overall degradation process (Liang et al., 2023). For example, persulfate has been shown to enhance the dissociation of PFOA, resulting in higher mineralization rates compared to processes without oxidants. Moreover, oxidants help reduce the recombination of photogenerated electrons and holes in photocatalytic systems, enabling more electrons and holes to participate in degradation reactions, further improving mineralization (Liu et al., 2022c; Yin et al., 2016). Oxidants also facilitate the sequential degradation of PFAS into shorter-chain perfluorinated acids, which are more easily mineralized, improving overall efficiency. When combined with photocatalysts, oxidants can lead to synergistic effects, as demonstrated by the use of phosphotungstic acid with UV light, which has shown improved PFAS mineralization in water treatment. These strategies underscore the importance of photochemical oxidants in optimizing photocatalytic processes for environmental remediation (Verma et al., 2024).

The application of photochemical oxidants has gained considerable attention for the degradation of recalcitrant contaminants, such as PFAS, which are resistant to conventional treatment methods. Uwayezu et al. (2023) found that combining ultraviolet (UV) light at 185 and 254 nm with persulfate effectively degrades PFAS by breaking the carbon-fluorine bonds. This approach generates reactive sulfate radicals, facilitating the breakdown of PFAS into less harmful by-products in both controlled and real-world water samples. However, the presence of competing contaminants, such as nitrate and chloride, reduces degradation efficiency by scavenging sulfate radicals. These findings highlight the importance of optimizing persulfate concentrations and operational parameters to enhance performance in complex wastewater matrices (Jean Noel Uwayezu, 2023). Esfahani and Mohseni (2022) investigated PFOS degradation using vacuum

ultraviolet (VUV) irradiation combined with a fluence-based approach, quantifying degradation by total energy absorbed (Table 3.1). VUV irradiation at 185 and 254 nm generated high-energy photons, breaking C-C and C-F bonds with hydrated electrons (e_{aq}^-) playing a key role. The addition of sulfite enhanced degradation rates, while advanced mass spectrometry analyses revealed wavelength-specific effects, with 185 nm improving fluorine recovery. Optimizing parameters such as sulfite concentration, pH, and dissolved oxygen further enhanced system efficiency. These findings highlight the potential of photochemical oxidation for PFAS remediation and the need for parameter optimization in complex matrices (Fig.3.2a) (Banayan Esfahani and Mohseni, 2022).

3.3.2 Semiconductor-Based Photocatalysis

Semiconductors have emerged as pivotal materials for photocatalytic degradation of PFAS, attributed to their distinct electronic properties and tunable characteristics (Mills et al., 1993). A semiconductor's bandgap, defined as energy differential between its conduction and valence band, is a key determinate of its photocatalytic performance (Wang et al., 2014). Optimizing the bandgap facilitates efficient electron excitation under light irradiation, leading to the formation of reactive species essential for PFAS degradation. This can be achieved through precise modifications to the semiconductor's size, structure, and composition, enabling enhanced photocatalytic activity.

Upon light activation, semiconductors generate electron-hole pairs, which interact with water and oxygen molecules to produce ROS, such as hydroxyl radicals and superoxide ions. These ROS play a critical role in cleaving the robust carbon-fluorine bonds present in PFAS molecules. Moreover, the incorporation of metal nanoparticles, such as silver, into semiconductor frameworks enhances photocatalytic performance by introducing electron traps and facilitating increased ROS

production. Nanostructured metal oxides with reduced bandgaps, such as indium oxide (In_2O_3), extend light absorption into a broader spectrum, further improving photocatalytic activity under diverse irradiation conditions. Additionally, the introduction of foreign metals on semiconductor surfaces promotes charge carrier separation, minimizing electron-hole recombination and sustaining the photocatalytic process, ultimately resulting in more efficient PFAS degradation (Bouteh et al., 2023; Verma et al., 2024; Xia et al., 2022).

Recent studies have highlighted the potential of semiconductor-based photocatalysts in addressing PFAS degradation. For example, Junying et al. (2023) synthesized Fe-doped zeolite via a wet-impregnation method using zeolite β, followed by drying and calcination at 500 ^oC, and then investigate its efficacy in PFAS degradation under UV light (Fig.3.2b). The Fe-doped zeolite demonstrated complete degradation of PFOA and PFOS within seven hours, while GenX exhibited a lower removal rate of 79%. The defluorination efficiencies varied, with PFOA achieving 69%, PFOS 51%, and GenX 33%. Although the results for PFOA and PFOS were promising, the reduced performance against GenX underscores the need for further optimization to target more recalcitrant PFAS compounds (Wen et al., 2023a). These findings emphasize the potential of semiconductor-based photocatalysts as effective tools for PFAS remediation, while also highlighting the necessity for continued research to enhance their performance against diverse PFAS structures.

Fan Li et al. (2020) developed a photocatalyst composite, Fe/TNTs@AC, combining iron-modified titanate nanotubes (TNTs) with activated carbon (AC) for efficient PFOA degradation (Fig.3.2c). The "concentrate-&-destroy" approach concentrates PFAS on the material's surface, accelerating UV-driven degradation. The catalyst degraded over 90% of PFOA within 4 hours, with 62% converted into fluoride ions. It also demonstrated self-regeneration, maintaining

performance over multiple cycles. The study emphasized key degradation mechanisms, including hole oxidation and C-F bond cleavage, offering an efficient and sustainable solution for PFAS treatment (Li et al., 2020).

A study by Qanbarzadeh et al. (2023) investigated hexagonal boron nitride (hBN) as a photocatalyst for PFAS degradation, hBN adsorbs PFAS mainly via hydrophobic interactions rather than electrostatic forces and this interaction is crucial because it allows for the effective clustering of PFAS molecules on the hBN surface, facilitating their degradation. hBN achieved over 99% PFOA degradation in 15 minutes and 65% PFOS degradation in one hour using a 5 L UVC/VUV photoreactor under realistic water conditions, outperforming previous photocatalysts (Qanbarzadeh et al., 2023) (Table 3.1). Duan et al (2020) explored boron nitride (BN) for PFOA degradation under UVC light, despite its wide band gap being considered a limitation (Fig.3.2d). Remarkably, BN outperformed TiO_2, achieving degradation rates up to four times higher. This success was linked to a hole-initiated reaction pathway and surface defects introduced by ball milling, enhancing UVC light absorption. BN efficiently degraded PFOA, releasing 52% of fluorine as fluoride ions in 240 minutes and maintained performance over multiple cycles unlike TiO_2. In simulated drinking water, BN achieved a 60% PFOA degradation rate, demonstrating practical potential. These findings highlight the promise of photocatalysts like Fe-doped zeolite, Fe/TNTs@AC, and BN while emphasizing the need for innovations in material design and process optimization to tackle real-world water treatment challenges (Duan et al., 2020).

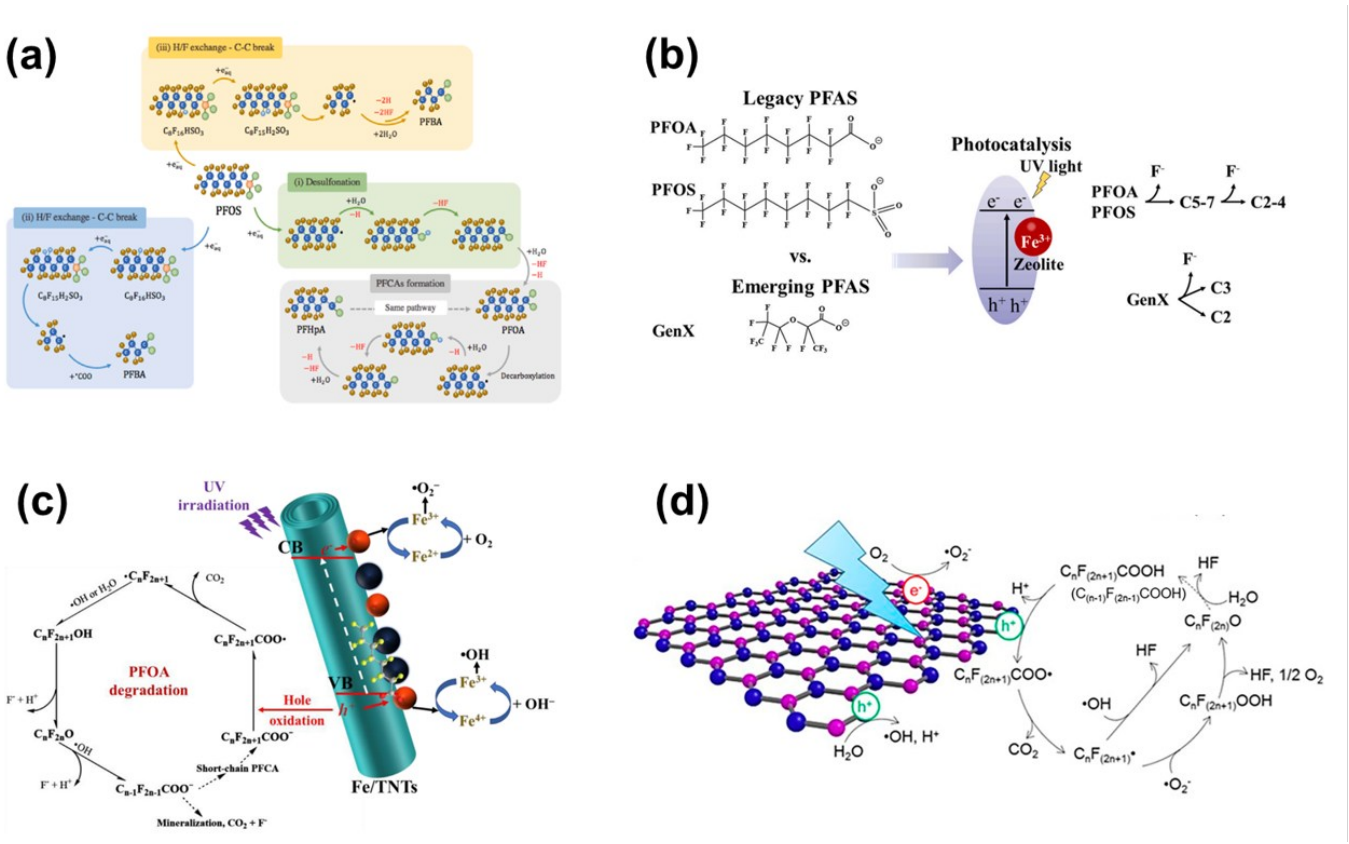

Figure 3.2 Various photo catalyst for PFAS removal (a) sulfite-mediated photolysis (Ehsan BE and M, 2022), (b) Fe-doped zeolite (Luo et al., 2024b), (c) Fe/TNTs@AC (Li et al., 2020), (d) BN (Duan et al., 2020).

3.3.3 Nanocomposite and Hybrid Photocatalysts

Recent advancements in the development of photocatalysts, particularly those based on nanocomposites and microparticles, have demonstrated significant improvements in the degradation of PFAS compared to conventional photocatalytic materials (Yin and Villagrán, 2022; Zhang et al., 2019b).

Nanocomposites enhance photocatalytic activity through a combination of their structural, electronic, and material-specific characteristics. Their elevated surface area-to-volume ratio increases the density of active sites, thereby facilitating more efficient adsorption of PFAS and consequently enhancing degradation rates. Furthermore, these nanomaterials effectively promote

the separation of photogenerated electron-hole pairs, minimizing charge recombination and enabling a greater number of reactive species to participate in the degradation process (Cardoso et al., 2023b; Raaja Rajeshwari et al., 2022).

The bandgap of nanocomposites can be precisely engineered to optimize absorption within the UV light spectrum, thereby further enhancing photocatalytic activity. The incorporation of multiple components, such as metal oxides with narrower bandgaps, induces synergistic effects that enhance overall reactivity. Additionally, structural modifications, including the use of nanoplates and porous microspheres, improve light absorption and increase the utilization of photon energy, thereby contributing to greater photocatalytic efficiency (Verma et al., 2024; Zhang et al., 2019b). Beyond their catalytic performance, nanocomposites exhibit exceptional stability and robustness, reducing the potential for material degradation and ensuring sustained efficacy in real-world applications (Mahpishanian et al., 2024). These properties render them highly suitable for large-scale environmental remediation, particularly in the degradation of persistent pollutants such as PFAS. Further research into the optimization and functionalization of nanocomposites is essential to fully exploit their potential in advancing PFAS treatment technologies.

3.3.4 Metal Oxide and Oxyhalide Systems

Microparticles are essential for enhancing photocatalytic efficiency, particularly in the degradation of persistent pollutants such as PFAS. The primary advantage of using microparticles lies in their increased surface area, which provides more active sites for photocatalytic reactions. This larger surface area facilitates more effective interactions between the photocatalyst and pollutants, thereby improving degradation rates. For instance, microparticles such as bismuth oxyhydroxphosphate ($Bi_3O(OH)(PO_4)_2$) have demonstrated degradation rates for PFOA that are

approximately 15 times higher than those achieved by conventional catalysts (Sahu et al., 2018). In addition to accelerating reaction rates, microparticles also offer enhanced stability and reusability, making them suitable for continuous photocatalytic processes. Their solid form enables easy recovery and reuse, which is particularly beneficial for large-scale applications. Furthermore, microparticles can be engineered to optimize their light absorption properties, increasing their effectiveness under natural sunlight by improving visible light capture. In addition, microparticles can serve as support structures for other catalytic materials, such as nanostructured or metal-doped catalysts, leading to the creation of composite photocatalysts that exhibit superior performance in PFAS degradation (Humayun et al., 2022). TiO_2 is a widely used photocatalyst for degrading PFAS, particularly PFOA, due to its availability and efficiency under UV irradiation (Guo et al., 2019; Park et al., 2018). Its primary mechanism involves generating electron-hole pairs via the photo-redox pathway, driving redox reactions that break down PFOA into less harmful byproducts. Charge-transfer mechanisms further enhance the interaction between TiO_2 and PFAS, promoting degradation (Haghighi et al., 2022; Schneider et al., 2014; Yao et al., 2021).

The efficiency of bulk TiO_2 is limited by rapid recombination of electron-hole pairs, reducing reactive holes necessary for effective photocatalysis. Modifications such as metallic nanoparticle doping (e.g., Ag, Pd, Pt) improve electron trapping and suppress recombination, significantly enhancing activity (Zhao et al., 2024). Similarly, hybridizing TiO_2 with carbon-based materials improves adsorption properties and electron-hole pair stability, boosting performance. Despite challenges, TiO_2 remains a key candidate for PFAS remediation, with ongoing efforts to optimize its properties (Huu-Tuan Do and Chao-Wei Huang, 2020).

Recent studies highlight the potential of modified TiO_2. A TiO_2-reduced graphene oxide (rGO) composite achieved a PFOA removal rate of 93 ± 7% after 12 hours of UV-vis irradiation,

quadrupling pure TiO_2 performance. Reduced band gap energy (3.2 eV to 2.72 eV), enhanced light absorption, and efficient charge separation facilitated by rGO contributed to this improvement. ROS generated during the process effectively mineralized PFOA, achieving 60% total organic carbon (TOC) reduction (Gomez-Ruiz et al., 2018) (Fig.3.3a).

Other advancements include mixed metal oxide (MMO)- TiO_2 composites, achieving 95.99 ± 1.49% PFOA removal under visible light through enhanced ROS generation and suppressed recombination (Yang et al., 2024). Titanium-based MOF MIL-177-HT showed 83% PFOA removal with 32% defluorination in 24 hours, though challenges in adsorption site accessibility and stability persist (Wen et al., 2023b) (Fig.3.3b).

Lead-doped TiO_2 with rGO (TiO_2-Pb/rGO) demonstrated 98% PFOA removal within 24 hours under UV light. Lead doping introduced oxygen vacancies for electron trapping, while rGO improved light absorption and adsorption properties (Chowdhury and Choi, 2023). BiOCl/ TiO_2 heterojunctions achieved complete PFOA degradation within 8 hours and 82% defluorination, leveraging efficient charge carrier separation and stability over cycles (Liu et al., 2022b) (Fig.3.3c). Additionally, BiOCl showed a defluorination efficiency of 59.3% under UV irradiation within 24 hours. Oxygen vacancies promoted electron-hole separation, while direct hole oxidation generated radicals for PFOA degradation. High reusability further underscores its practical potential (Song et al., 2017).

These advancements emphasize the progress in TiO_2-based photocatalysts for PFAS remediation, paving the way for efficient and scalable photocatalytic water treatment solutions. Recent studies have advanced the use of indium oxide (In_2O_3) and gallium oxide (Ga_2O_3) as photocatalysts for the degradation of PFOA, a key contaminant in PFAS (Chang et al., 2022; Habib et al., 2023; Li et al., 2013). A MnO_x-modified, oxygen-vacancy-rich In_2O_3 submicro-rod photocatalyst (MnOx/

In_2O_3-Ov SR) has been developed for enhanced PFOA removal. The incorporation of manganese oxide increases the surface area, adsorption capacity, and photocatalytic activity under solar light irradiation, resulting in improved degradation and defluorination efficiencies. This enhancement is attributed to the increased generation of ROS, such as hydroxyl and superoxide radicals, essential for pollutant breakdown (Yaoyao Wu, 2019).

Gallium oxide (Ga_2O_3) has also been explored as a stable, non-toxic photocatalyst for aqueous PFOA treatment, surpassing traditional catalysts like titanium dioxide (TiO_2). A Ga_2O_3-peroxymonosulfate (PMS) system, activated by UV light, produces sulfate radicals ($SO_4^{\bullet -}$), significantly enhancing degradation efficiency. Under optimal conditions (UV irradiation at 185 nm, pH 3), this system achieves complete PFOA degradation within 60-90 minutes. Mechanistic studies reveal stepwise degradation of PFOA to shorter-chain intermediates, such as perfluoroheptanoic acid (PFHpA) and perfluorohexanoic acid (PFHxA), driven by sulfate and superoxide radicals, with hydroxyl radicals assisting. Notably, the system demonstrates a TOC removal rate of 75-85%, highlighting its practical potential for wastewater treatment (Xu et al., 2020) (Fig.3.3d).

Building on previous research, a nanostructured, sheaf-like Ga_2O_3 photocatalyst was synthesized through a polyvinyl alcohol (PVA)-assisted hydrothermal method followed by heat treatment. This morphology provides a high specific surface area (36.1 m^2/g) and nanoporous structure, enhancing interaction with PFOA molecules. The sheaf-like Ga_2O_3 exhibited a decomposition rate constant of 4.85% h^{-1} under 254 nm UV irradiation, with efficiencies 16 times greater than commercial Ga_2O_3 and 44 times higher than P25 TiO_2. Under vacuum UV (VUV) irradiation at 185 nm, the catalyst effectively removed trace PFOA from secondary effluents, overcoming interference from organic matter and bicarbonate in wastewater. The photocatalyst

displayed excellent stability and reusability, maintaining high efficiency over multiple cycles, positioning it as a promising candidate for PFAS removal in water treatment (Shao et al., 2013). Similarly, a Bi_4O_7-modified Ga_2O_3 composite (GaBi10) was developed to improve photocatalytic efficiency for PFOA degradation. The GaBi10 composite exhibited enhanced light absorption, charge carrier separation, and adsorption capacity. Compared to pure Ga_2O_3, which achieved only 5.82% degradation, GaBi10 demonstrated a significantly higher defluorination rate of 59.6%, effectively breaking down the C-F bonds in PFOA. Despite a lower mineralization rate (TOC reduction of 64.1%), these results suggest that intermediate products hinder complete mineralization. The GaBi10 composite outperformed previous catalysts in degradation, defluorination, and mineralization. However, variations in experimental conditions across studies pose challenges for standardizing performance comparisons. This research emphasizes the importance of optimizing catalyst design and experimental parameters to advance the photocatalytic degradation of PFAS pollutants, like PFOA, and improve environmental remediation strategies (Chen et al., 2024).

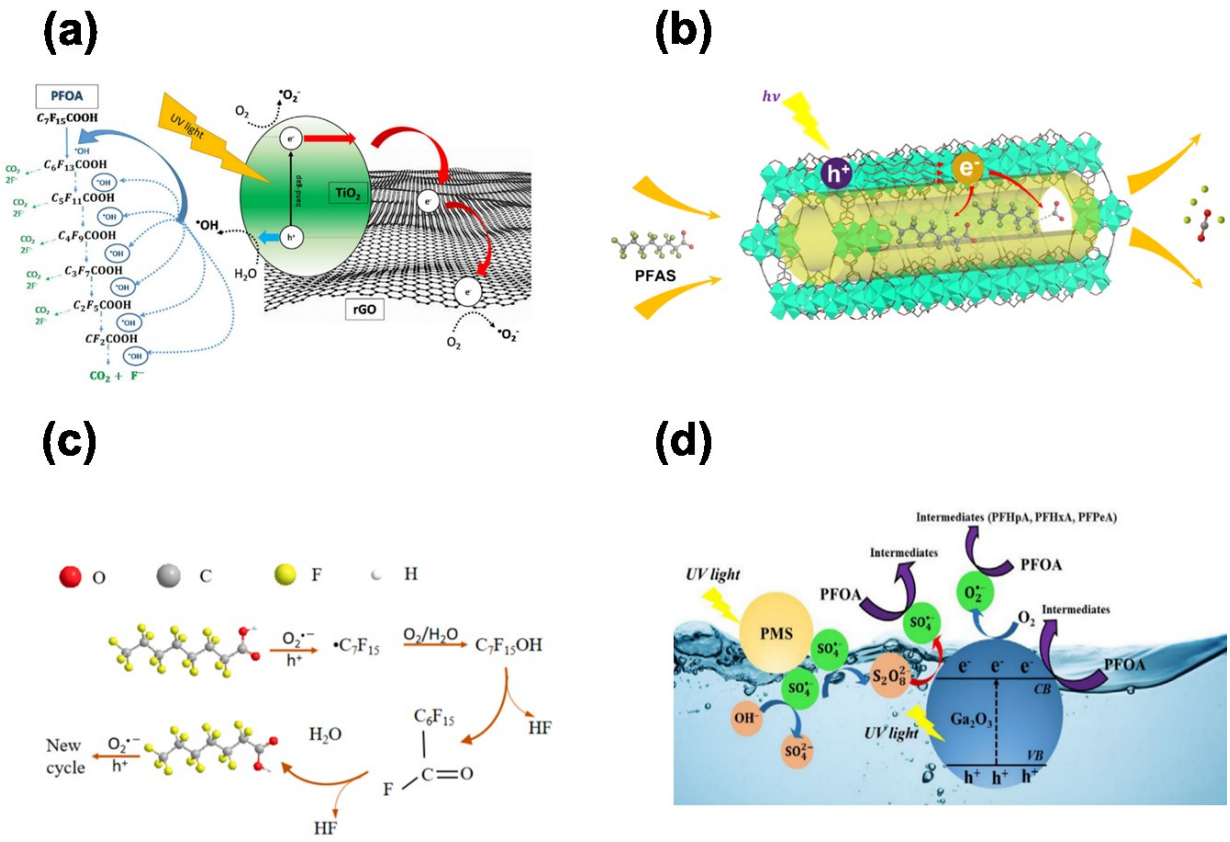

Figure 3.3 Advanced nanomaterials for enhanced photocatalytic PFAS removal (a) TiO_2-rGO catalyst (Gomez-Ruiz et al., 2018), (b) MIL-177-HT (Wen et al., 2023b), (c) $BiOCl/TiO_2$ (Liu et al., 2022b), (d) Ga_2O_3-PMS (Xu et al., 2020).

3.3.5 Coupled and Advanced Photocatalytic Systems

Photocatalytic ozonation for the removal of five PFAS (PFOA, PFHxS, PFBS, 6:2 FTS, and GenX) from water using a WO_3/TiO_2 catalyst under UVA-visible light was investigated (Brent Lashuk, 2022) (Table 3.1). Four catalysts with varying WO_3 content (0%, 1%, 3%, and 5% by weight) were synthesized via the sol-gel method and characterized through XRD, TEM, STEM-EDS, HAADF-STEM, N_2 adsorption/desorption isotherms, and DRS-UV-vis. The 5 wt% WO_3/TiO_2 catalyst demonstrated the highest photocatalytic activity, as assessed using methylene blue. Despite this, the photocatalytic ozonation process resulted in only 16% total PFAS removal

(ranging from 4% to 26%) after 4 hours of UVA-visible light exposure. Photocatalysis alone achieved a similar removal rate, while photolysis and ozone photolysis were less effective, and ozonation alone showed no effect. Microtox analysis confirmed that both photocatalysis and photocatalytic ozonation treatments eliminated initial acute toxicity. The low PFAS removal efficiency under the tested conditions suggests that future studies should focus on optimizing catalysts and treatment conditions. The variability in removal rates among different PFAS highlights the importance of evaluating a range of compounds in future investigations. This study introduces WO_3/TiO_2 catalysts for photocatalytic ozonation, contributing to the development of catalytic processes for the removal of persistent environmental pollutants and advancing the understanding of photocatalytic processes in environmental pollution control (Brent Lashuk, 2022).

Photo-membrane reactor (PMR) technology has recently gained significant attention as another solution for the removal of PFAS contaminants, surpassing traditional water treatment methods in effectiveness. The PMR system demonstrated a significant advantage, achieving up to 80% removal of PFOA within the first two hours of operation. Over two 8-hour cycles, PMR maintained an average removal rate of 69%, significantly outperforming traditional methods, which typically achieve removal rates of less than 25% using techniques such as ultrafiltration (UF). A key benefit of PMR technology is its operation at lower transmembrane pressures, averaging less than 1 bar, in contrast to higher pressure methods such as reverse osmosis (RO) and nanofiltration (NF). This lower pressure requirement not only improves energy efficiency but also enhances the sustainability of the PMR system by reducing energy consumption. Furthermore, PMR technology minimizes waste generation by integrating adsorption and photocatalytic degradation processes, reducing the environmental impact associated with traditional methods, such as the generation of concentrated brines.

PMR has also demonstrated significant capability in degrading PFAS contaminants in situ, achieving a 95% destruction rate for adsorbed PFOA. In contrast, traditional methods typically focus on PFAS removal without addressing degradation, which may leave harmful residues in the treated water. PMR has proven its effectiveness in treating mixed PFAS solutions, with removal rates of 35% for PFOA and 46% for PFOS, indicating its adaptability in handling complex mixtures of contaminants, a challenge for many conventional treatment technologies (Junker et al., 2024). This study shows the ability of PMR technology to both remove and degrade PFAS contaminants, offering a more sustainable and efficient approach for PFAS remediation and wastewater treatment.

Table 3.1 Summary of recent photocatalytic PFASs degradation

Photocatalyst	PFAS Target	$[PFAS]_0$	Other conditions	Degradation Efficiency	Ref
UV/VUV/SO_3^{2-}	PFOS	100 ppb	DO = 0.14 mg/L, solution pH = 12.0, and temperature 22 ± 2 ℃	85% (6h)	(Banayan Esfahani and Mohseni, 2022)
Fe-zeolite	GenX, PFOA, PFOS	10 μM	with 1 g/L Fe-zeolite, from 4.44 to 4.98 to 3.88–4.58	GenX (79%), PFOA (100%), PFOS (100%) 7 h	(Wen et al., 2023a)
Fe/TNTs@AC	POFA		(254 nm, 21 mW/cm^2), pH range of 4–8	90% (4 hours),	(Li et al., 2020)
Hexagonal boron nitride (hBN)	POFA, POFS	PFOA = 50 μg/L PFOS = 50 μg/L	(pH=4) UV lamp(185/254 nm)	99% (15 min), 65% of PFOS (1 hour),	(Qanbarzadeh et al., 2023)
Boron nitride (BN)	PFOA, GenX	50 mg/L	254 nm irradiation, 2.5 g of BN/L, pH=3	60% to 80% degradation (120 min)	(Duan et al., 2020)
TiO_2-Pb/rGO	PFOA		0.1 g/L of TiO_2-rGO	93 ± 7% (12 hours),	(Gomez-Ruiz et al., 2018)
MMO-TiO_2	PFOA	300 mg/L	1 g/L of catalyst, pH=3	95.99 ± 1.49% PFOA	(Yang et al., 2024)
MIL-177-HT	PFOA	100 μg/L	TEOA v/v% = 5.0%; MOF loading = 2.5 g/L; T = 20°C	83% (24 hours)	(Wen et al., 2023b)
TiO_2-Pb/rGO	PFOA	10 mg/L	0.33 g/L photocatalyst, PH= 4.5 to 7.5	98%, (24hours)	(Chowdhury and Choi, 2023)
BiOX/TiO_2 (BiOI/TiO_2, BiOBr/TiO_2 and BiOCl/TiO_2)	PFOA		catalyst dosage: 0.2 g/L 254 nm UV light	88%, 100% and 96%, respectively (8 hours)	(Liu et al., 2022b)
Bismuth oxychloride (BiOCl)	PFOA			59.3% defluorination efficiency (24 hours)	(Song et al., 2017)
MnOx/In_2O_3-Ov SR	PFOA	50 mg/L	4% MnOx/In_2O_3, 500 W Xe lamp,	99.8% (3h)	(Yaoyao Wu, 2019)

			Catalyst concentration: 0.5 g/L pH=3.8		
Ga_2O_3 peroxymonosulfate (PMS)	PFOA	50 ng/L - 50 mg/L	pH=3, 254 nm and 185 nm UV irradiation	100% PFOA (60 to 90 minutes),	(Xu et al., 2020)
Bi_4O_7-modified Ga_2O_3 composite (GaBi10)	PFOA			5.82% PFOA	(Chen et al., 2024)
WO_3/TiO_2	PFOA, PFHxS, PFBS, 6:2 FTS, GenX	250 μg/L for each	0.2 g/L of catalyst neutral pH	16% total removal, ranging from 4% to 26% (4 hours)	(Brent Lashuk, 2022)
Photo-membrane reactor (PMR)	PFOA, Mixed (PFOS, POFA)			Average removal rate of 69% (two cycles of 8 hours) Mixed (35% for PFOA and 46% for PFOS)	(Junker et al., 2024)

3.4 Key Challenges and Knowledge Gaps

Photocatalytic degradation of PFAS faces several challenges that hinder its practical application. One primary issue is the low conversion efficiency of many semiconductor photocatalysts, particularly under visible light. This limitation is significant because sunlight, a major energy source, is essential for large-scale photocatalytic processes. However, most commonly used photocatalysts, such as TiO_2, are only active under UV light, which renders them less suitable for solar-driven PFAS degradation. Although efforts to develop new materials and strategies to enhance photocatalytic efficiency under visible light are ongoing, practical solutions have yet to be fully realized.

Another major challenge is the rapid recombination of photogenerated electron-hole pairs, which reduces the availability of active species necessary for PFAS degradation. When a

photocatalyst absorbs light, electron-hole pairs are generated, producing reactive species like hydroxyl radicals that facilitate the breakdown of PFAS. However, rapid recombination of these pairs leads to the loss of many reactive species, reducing the degradation rate, particularly for compounds like PFOA that are highly resistant to breakdown due to their stable chemical structure. Moreover, the inefficient transport and separation of photogenerated carriers in many photocatalytic systems further diminish their effectiveness.

The complexity of PFAS degradation is compounded by competitive adsorption, where other ions or compounds in water compete with PFAS for adsorption sites on the photocatalyst surface. For instance, bicarbonate ions can block active sites, reducing the efficiency of PFAS degradation. This is particularly problematic in real-world environments, where water often contains multiple contaminants. Moreover, environmental factors such as pH significantly influence photocatalytic processes. Alkaline conditions, in particular, can hinder PFAS adsorption onto the photocatalyst surface, lowering degradation rates. Maintaining optimal conditions across diverse environments remains a challenge, affecting the consistency of results in different water treatment scenarios.

Another inherent difficulty in photocatalytic PFAS degradation is the chemical stability of PFAS compounds due to their strong carbon-fluorine (C-F) bonds. These bonds cause PFAS molecules highly resistant to conventional degradation methods, posing a significant challenge for photocatalysis. Efficient degradation requires the generation of highly reactive species capable of breaking these stable bonds. However, the breakdown products of PFAS need to be carefully monitored, as they could potentially be more harmful than the original compounds. Ensuring that degradation by-products are less toxic is crucial for the safe application of photocatalytic methods.

Lastly, although photocatalytic degradation has shown promising results in laboratory studies, scaling up these technologies for practical, large-scale applications remains challenging. The energy requirements for photocatalytic processes, especially when artificial light is necessary, can be prohibitively high. Moreover, the need for efficient photocatalyst regeneration and prevention of deactivation complicates the feasibility of large-scale deployment. The high costs associated with materials and operational demands also raise concerns about the scalability and economic viability of photocatalytic PFAS degradation for widespread environmental use (Luo et al., 2024a).

3.5 Future Research Directions and Emerging Opportunities

Photocatalytic degradation of PFAS has emerged as a promising approach for environmental remediation, yet several critical challenges limit its practical application. A major limitation is the restricted absorption of visible light by conventional photocatalysts, such as TiO_2, which predominantly respond to UV light. Enhancing the ability of photocatalysts to utilize a broader portion of the solar spectrum remains a key priority for future research.

Another significant challenge lies in the inefficient utilization of photogenerated electron-hole pairs. Rapid recombination reduces the availability of charge carriers for PFAS degradation, highlighting the need for strategies that improve charge separation and transport. Sustainability concerns also arise due to the reliance on heavy metals in many photocatalysts, which may pose environmental and toxicity risks in large-scale applications. Future research should explore alternative materials that balance efficiency with environmental safety, durability, and reusability (Ma et al., 2022).

Additionally, real-world water matrices present complexity that is often not captured in laboratory studies. Natural organic matter and other coexisting substances can impede photocatalytic activity,

suggesting that hybrid or integrated treatment approaches may be necessary to ensure effectiveness under practical conditions.

Finally, a deeper understanding of the degradation mechanisms, including the formation and fate of intermediates, is essential to optimize photocatalytic processes. Research that addresses efficiency, sustainability, and real-world applicability will be critical for advancing PFAS remediation technologies (Chen et al., 2023; Liu et al., 2022a; Luo et al., 2024a; Verma et al., 2024).

3.6 Summary and Relevance to This Thesis

This chapter has provided a comprehensive review of recent advancements in photocatalytic PFAS degradation, emphasizing fundamental principles, emerging photocatalyst materials, and innovative strategies including photochemical oxidants, semiconductor based photocatalysis, nanocomposites, and integrated systems such as photo membrane reactors and ozonation. Critical insights into the mechanisms of PFAS degradation, including electron hole generation, reactive oxygen species formation, and carbon fluorine bond cleavage, have been highlighted to elucidate the structure performance relationships that govern catalyst efficiency.

Building on the challenges and opportunities discussed in Section 3.5, key limitations identified in previous studies include limited absorption of visible light, rapid recombination of photogenerated carriers, competition from coexisting water constituents, incomplete mineralization of PFAS, formation of potentially toxic intermediates, and scalability constraints. Despite advances in catalyst design, such as heterojunction formation, metal or nonmetal doping, nanostructuring, and hybrid composite materials, these limitations continue to restrict overall degradation efficiency and practical applicability.

The gaps revealed by this review, particularly insufficient visible light activity, rapid charge carrier recombination, and incomplete PFAS mineralization, underscore the necessity for the development of new photocatalytic materials with optimized properties. Addressing these deficiencies is essential to achieve more efficient, selective, and sustainable PFAS removal under environmentally relevant conditions. Motivated by these findings, the present study focuses on the design and evaluation of novel photocatalysts that enhance light absorption, promote charge separation, and maximize degradation efficiency while minimizing the formation of harmful intermediates. This approach directly stems from the mechanistic insights and performance limitations identified in the reviewed literature, establishing a clear rationale for the subsequent experimental investigations.

Chapter 4: Optimized Cu_2S Photocatalysts for Highly Efficient Removal of PFAS from Aqueous Solutions

4.1 Introduction

PFAS, including PFOA and PFOS, are persistent contaminants frequently detected near industrial sites such as airports, textile facilities, and metal smelters (Aditi et al., 2021; Kotthoff et al., 2015; Zareitalabad et al., 2013). Their extreme chemical stability and resistance to degradation allow them to accumulate in aquatic systems, where they pose documented ecological and human-health risks (Jain, 2013; Liu et al., 2023; Sadia et al., 2023). Major sources, including aqueous film-forming foams, non-stick coatings, and industrial effluents, continue to introduce PFAS into water resources, reinforcing the need for effective and sustainable remediation technologies (Podder et al., 2021; Tabatabaei et al., 2025). Conventional treatment methods such as activated carbon adsorption, ion exchange, and membrane filtration can remove PFAS from water but do not mineralize them, often generating secondary waste streams and incurring high operational costs (Tabatabaei et al., 2025). Catalytic degradation, particularly photocatalysis, offers a more sustainable path by enabling direct destruction of PFAS under mild conditions. Yet photocatalytic PFAS degradation remains challenging due to the high C–F bond dissociation energy and the limited redox capacity of conventional photocatalysts. TiO_2, for example, requires UV light (3–5% of solar energy), exhibits rapid electron–hole recombination, and shows low activity toward PFOA. Other semiconductors such as Ga_2O_3, In_2O_3, and g-C_3N_4 face similar limitations (Chang et al., 2022; Chen et al., 2024; Tabatabaei et al., 2025).

Although visible-light-responsive systems including BiOX (Br, I) offer improved solar utilization, further enhancement in photostability and reductive power is necessary for efficient C–F activation

(Liu et al., 2022b; Tabatabaei et al., 2025). Nanostructuring strategies, via tuning particle size, shape, and morphology, have been effective in improving charge separation (Cardoso et al., 2023a), yet materials capable of delivering the strong, sustained reducing electrons needed for PFAS mineralization remain scarce.

Copper sulfides are costly effective materials which have recently gained attention as promising candidates to address these limitations. Their tunable stoichiometry, broad visible–NIR absorption, high conductivity, and intrinsic defect chemistry enable strong reductive potentials and efficient charge transport under solar irradiation. Cu_2S-based nanomaterials have demonstrated high performance in degrading dyes and antibiotics (Ait-Karra et al., 2023; Wang et al., 2022; Xu et al., 2015) , highlighting their potential applicability to PFAS degradation.

Among copper sulfides, Cu_2S is particularly compelling due to its narrow band gap, high carrier mobility, and capacity for Cu^+/Cu^{2+} redox cycling at sulfur-coordinated sites. These features can generate strongly reducing electrons capable of initiating C–F bond scission through direct electron transfer or radical-mediated pathways not accessible with typical oxide photocatalysts (Cao et al., 2024; Cardoso et al., 2023a; Zelekew et al., 2024). Additionally, vacancy-rich Cu_2S lattices may stabilize reactive intermediates and promote continuous electron flow, making Cu_2S a rational and targeted choice for addressing the mechanistic challenges inherent in PFAS photocatalysis (Cao et al., 2024; Guo et al., 2020).

This study examines CuS, Cu_2S, and mixed-phase $Cu_2S3/2$, along with Cu_2S supported on reduced graphene oxide (rGO), synthesized through hydrothermal and solvothermal methods, for the photocatalytic degradation of PFOA and PFOS under UV irradiation. The investigation is guided by three proposed mechanistic ideas. First, variations in the Cu(I)/Cu(II) ratio are expected to modulate electron-transfer pathways and, in turn, influence the extent of PFAS degradation.

Second, differences in phase purity between Cu_2S and $Cu_2S3/2$ are anticipated to affect the generation of reactive species during irradiation, producing distinct degradation behaviors. Third, incorporating rGO is proposed to enhance charge separation and suppress charge-carrier recombination relative to unsupported Cu_2S, yielding improved photocatalytic performance. Assessing these concepts clarifies the structure–function relationships governing copper-based sulfide photocatalysts and informs the development of scalable treatment strategies for emerging water contaminants.

4.2 Materials and Methods

4.2.1 Chemicals and Materials

All reagents were used as received without further purification. Copper(II) chloride dihydrate ($CuCl_2 \cdot 2H_2O$, 99%, Acros Organics), L-cysteine, sodium diethyldithiocarbamate, and methanol were employed for the synthesis of the copper-based particles. Sulfuric acid (H_2SO_4, 98%, Fisher Chemical), o-phosphoric acid (H_3PO_4, 85%, Fisher Chemical), graphite powder (325 mesh, Alfa Aesar), potassium permanganate ($KMnO_4$, 99%, J.T. Baker), hydrochloric acid (HCl, 36%, Fisher Chemical), and hydrogen peroxide (H_2O_2, 99%, J.T. Baker) were utilized in the preparation of graphene oxide. Ultrapure deionized water was used as the solvent in all experimental procedures. This delineation of materials ensures reproducibility and clearly differentiates the reagents employed for Cu_2S synthesis, graphene oxide synthesis, and subsequent reduction, thereby highlighting the specific function of each chemical in the fabrication of the nanocomposites.

4.2.2 Synthesis of Photocatalyst

4.2.2.1 Cu_2S and CuS Synthesis

The synthesis of Cu_2S was conducted via a hydrothermal method. Initially, 0.867 mmol of Cu^{2+} ions were dissolved in 40 mL of deionized water, followed by the addition of 0.619 mmol of cysteine, yielding a theoretical Cu^{2+}:S^{2-} molar ratio of 1.4:1. The resulting mixture was transferred to a Falcon tube and vigorously agitated at 3000 rpm for 1 min, producing a dark bluish dispersion. This dispersion was subsequently loaded into a 50 mL Teflon-lined stainless-steel autoclave and subjected to hydrothermal treatment at 185 °C for 6 h in a temperature-controlled oven. Upon completion, the resulting brownish precipitate was isolated by centrifugation at 5000 rpm for 2 min, washed with deionized water at least three times, and dried in a vacuum oven at 60 °C for 6 h. CuS was synthesized through a solvothermal approach using 200 mg $CuCl_2 \cdot 2H_2O$ (1.17 mmol), 200 mg sodium diethyldithiocarbamate, and 200 mg polyvinylpyrrolidone (PVP), all dissolved in methanol. The solution was transferred to a sealed reaction vessel and heated at 120 °C for 24 h. After cooling to room temperature, the product was collected by centrifugation, rinsed with water and ethanol, and dried under vacuum, following the same washing and drying procedures applied for Cu_2S (Dai et al., 2023; He et al., 2021; Zhang et al., 2020).

4.2.2.2. Cu_2S/CuS Synthesis

For the Cu_2S/CuS composite ($Cu_2S3/2$), 230 mg $CuCl_2 \cdot 2H_2O$ (1.35 mmol) and 100 mg sodium diethyldithiocarbamate were processed under identical solvothermal conditions as CuS, including the same purification and drying steps.

4.2.2.3 rGO Synthesis

Graphene oxide (GO) recovered after centrifugation was obtained as a gel, which was subsequently frozen at –30 °C for 24 h. The frozen material was then subjected to lyophilization using a Labconco freeze-drying system operating at 0.081 mbar and –38 °C, yielding a GO aerogel. For the preparation of reduced graphene oxide (rGO), GO (250 mg) was dispersed in 50 mL of deionized water and tip-sonicated for 10 min at 20% amplitude to achieve uniform exfoliation. Glucose (250 mg; mass ratio 1:1 relative to GO) was then introduced, followed by an additional 10 min of sonication to ensure homogeneous mixing. The resulting GO–glucose dispersion was transferred into 50 mL Falcon tubes, frozen at –20 °C for a minimum of 48 h, and subsequently freeze-dried under the same lyophilization conditions used for GO. The dried GO–glucose composite powder was thermally reduced in a tube furnace under flowing argon (30 sccm), preceded by a 30 min argon purge. The temperature was increased to 1000 °C at a rate of approximately 4.7 °C min^{-1} (total ramp time ≈3 h 30 min), held at 1000 °C for 3 h, and then allowed to cool naturally under argon to room temperature. The resulting rGO powder was finally tip-sonicated for 20 min at 20% amplitude to facilitate redispersion (Jing Li, 2019; Ramirez-Ubillus et al., 2023).

4.2.2.4. Preparation of Cu_2S–rGO Composite

Cu_2S powder was added to the rGO dispersion at a mass ratio of 3:1 (Cu_2S:rGO), and the mixture was further tip-sonicated for 20 min under the same conditions to obtain a homogeneous suspension. The resulting Cu_2S–rGO dispersion was centrifuged at 5000 rpm for 5 min, the supernatant was discarded, and the solid composite was dried in a vacuum oven at 50 °C for at

least 6 h. The dried Cu_2S–rGO composite was then collected and stored for subsequent experiments (Dai et al., 2023; He et al., 2021; Ramirez-Ubillus et al., 2023).

4.2.3 Characterization of Photocatalysts

Three copper sulfide–based photocatalysts were synthesized at the NanoScience Technology Center and the Department of Chemistry at the University of Central Florida with the aim of controlling the Cu^+/Cu^{2+} ratio and fine-tuning the phase composition. The Cu^+/Cu^{2+} distribution in each sample was quantified using X-ray photoelectron spectroscopy (XPS). Additional characterization techniques, including scanning electron microscopy (SEM), energy-dispersive X-ray spectroscopy (EDS), and Raman spectroscopy, were employed to verify the synthesis pathways and confirm the structural and compositional features of the final materials. The first photocatalyst, CuS, was synthesized via a solvothermal method, while the second, Cu_2S, was prepared using a hydrothermal approach. A third material, a Cu_2S/CuS composite, was produced through a solvothermal route as described above. Finally, a Cu_2S–rGO composite was synthesized as a new coupled photocatalyst.

4.2.4 Photodegradation Experiment

For the photocatalytic degradation experiments, perfluorooctanoic acid (PFOA) and perfluorooctane sulfonate (PFOS) were selected as the target contaminants, each at an initial concentration of 1 mg/L. The synthesized photocatalysts included CuS, Cu_2S, and a mixture of Cu_2S/CuS. Additionally, a hybrid material was prepared by coating Cu_2S onto reduced graphene oxide (Cu_2S/rGO) to enhance photocatalytic performance. The reactions were conducted in a

closed photoreactor system equipped with a UV light source (wavelength range: 245–365 nm; power: 6 W). Experimental conditions were maintained at pH 4–5 with a catalyst dosage of 20 mg at room tempreture, reaction time of 8 hours, and room temperature. The reaction mixtures were stirred continuously at 350 rpm to ensure uniform dispersion of the photocatalysts. The degradation efficiency of PFOA and PFOS was monitored by measuring their concentrations using liquid chromatography-mass spectrometry (LC-MS, Agilent 1290 LC system coupled to a Thermo LTQ Orbitrap Velos mass spectrometer). This experimental setup enabled a systematic assessment of the photocatalytic performance of the synthesized copper-based materials under well-controlled conditions. All reactions were conducted using a hotplate magnetic stirrer (JOANLAB, ON) and a UV light source operating within a wavelength range of 245–365 nm with a power output of 6W, and the UV-irradiation experiments were carried out for a duration of 8 hours (Fig.4.1).

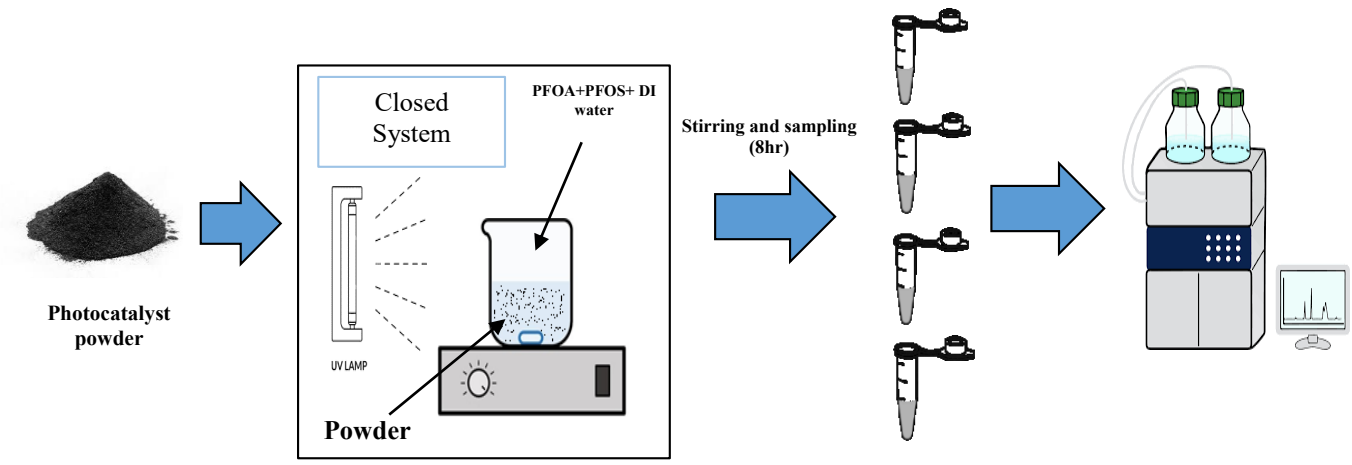

Figure 4.1 PFASs photodegradation experiment using photocatalyst powder in a closed photoreactor system equipped with a UV light source followed by LC-MS analysis

4.2.5. Analytical Methods

All samples were diluted tenfold and centrifuged as a pretreatment step prior to LC-MS analysis to determine PFOA and PFOS concentrations. MS analyses were performed on an Agilent 1290 LC system coupled to a Thermo LTQ Orbitrap Velos mass spectrometer equipped with a heated electrospray ionization (ESI) source operating in negative ion mode. Given the short retention time and direct MS detection, no analytical column was used; instead, the mobile phase (water/acetonitrile, 1:1 v/v, containing 0.1% formic acid) was delivered at a flow rate of 250 µL/min for 4 minutes per sample. A 5 µL injection volume was used, and MS spectra (m/z 200–800) were acquired in the Orbitrap at a resolution of 100,000. Internal calibration was performed using a background peak at m/z 311.1686 Da as a lock mass. PFOA and PFOS were monitored as $[M–H]^-$ ions at m/z 412.9664 and 498.9302, respectively. Peak intensities were reported as average values of MS scan #3–8 using Thermo XCalibur software (v2.2 SP1.48). An internal standard was included to improve quantification accuracy and reliability, and replicate measurements were performed by analyzing the same sample three times on the instrument to assess analytical precision.

The degradation efficiency of PFAS was calculated according to the following equation Eq. (1); where C_0 represents the initial PFAS concentration:

$$\text{Degradation efficiency (\%)} = (C_0 - C_t)/ C_0 \times 100 \qquad (1)$$

4.3 Results and Discussion

4.3.1 Characterization of Materials

4.3.1.1. SEM and EDS

The morphology of CuS, Cu_2S, and the Cu_2S/CuS composite was examined using scanning electron microscopy (SEM), as shown in Fig. 4.2. The CuS sample exhibited a distinct flower-like structure with an average size of approximately 3.5 μm (Fig. 4.2a). In contrast, the Cu_2S sample consisted of uniformly distributed nanoparticles with an average diameter of 110 nm (Fig. 4.2b). The Cu_2S/CuS composite displayed quasi-spherical particles with an average size of around 250 nm (Fig. 4.2c). To complement the morphological analysis, energy-dispersive X-ray spectroscopy (EDS) was conducted alongside SEM to qualitatively assess the chemical composition of the CuS, Cu_2S, and Cu_2S/CuS samples (Fig. 4.3.). As expected, both CuS and Cu_2S exhibited strong signals for copper (Cu) and sulfur (S), confirming the presence of these elements in their compositions. The observed carbon (C) and oxygen (O) signals are primarily attributed to the conductive carbon tape used for sample mounting. The EDS-derived elemental compositions (Table 4.1), revealed Cu/S molar ratios of 1.56 for CuS and 2.67 for Cu_2S, indicating a higher copper content in the latter. In the case of the Cu_2S/CuS composite, EDS spectra showed the presence of Cu, S, and nitrogen (N). The detection of nitrogen suggests incomplete decomposition of the sulfur precursor, diethyldithiocarbamate ($C_5H_{10}NS_2$), during the hydrothermal synthesis. The Cu/S molar ratio for this sample was 2.26, intermediate between the ratios observed for CuS and Cu_2S, supporting the presence of a mixed-phase structure. Additionally, nitrogen was present at approximately 3%, further indicating a minor residual fraction of the unreacted precursor (Kociołek-Balawejder et al., 2023; Lv et al., 2022).

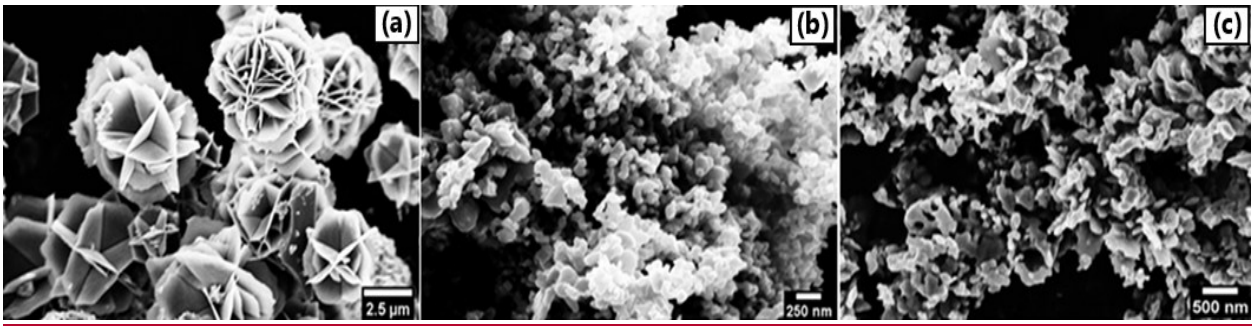

Figure 4.2 SEM images of a) CuS b) Cu_2S c) Cu_2S/CuS

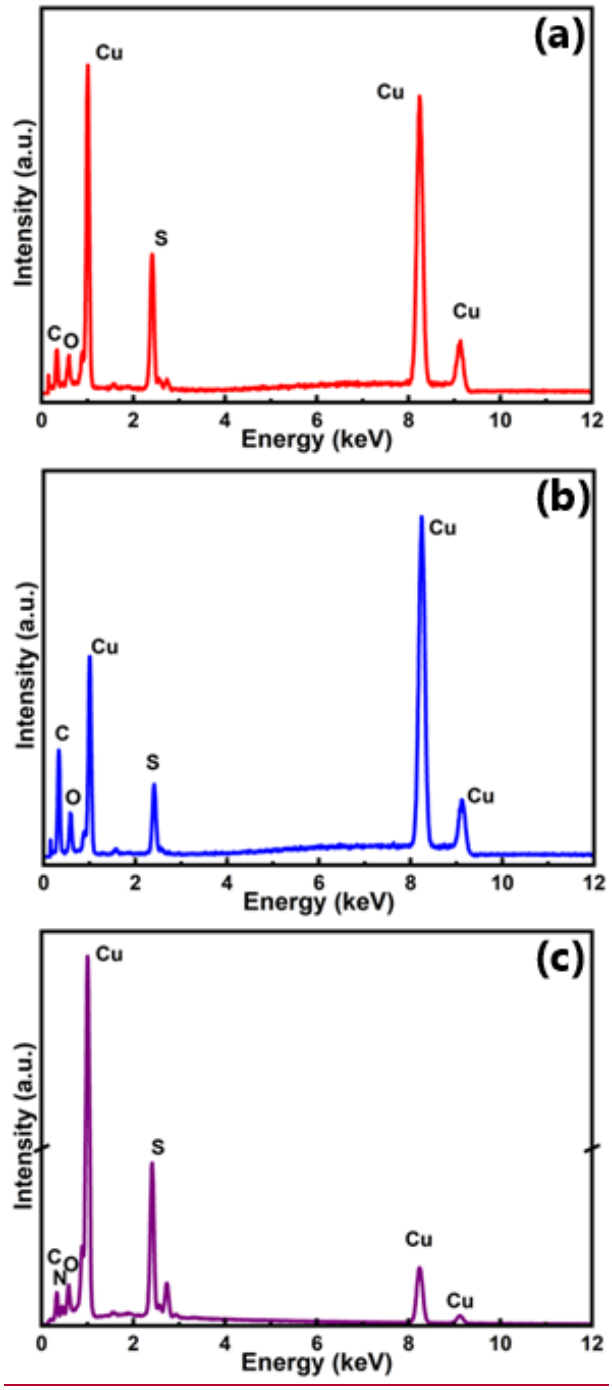

Figure 4.3 EDS spectra of CuS, Cu_2S, Cu_2S/CuS

Table 4.1 Atomic composition of the CuS, Cu_2S, Cu_2S/CuS quantified EDS study

Element	Atomic composition (%)		
	CuS	Cu_2S	Cu_2S/CuS
S	18.62	7.05	19.96
Cu	29.09	18.69	45.31
C	41.78	61.60	22.84
N	-	-	3.69
O	10.52	12.66	8.20

4.3.1.2 Morphological and Elemental Characterization of Cu_2S/rGO Composite

The surface morphology of the Cu_2S/rGO composite was analyzed using scanning electron microscopy (SEM), as illustrated in Figure 4.4. The micrograph shows a rough, porous structure composed of rGO flakes with partially stacked and wrinkled layers-features typical of restacked graphene after drying. Although high-energy sonication was employed during synthesis, some aggregation of the rGO sheets remained, forming micron-sized interconnected networks with numerous voids. Within these carbonaceous folds, uniformly dispersed nanocrystals, averaging about 110 nm in diameter, can be observed and are attributed to the embedded Cu_2S phase. The strong interfacial contact between Cu_2S nanoparticles and the rGO matrix is anticipated to improve electrical conductivity and offer abundant electrochemically active sites, as the conductive graphene framework facilitates efficient electron transfer between the Cu_2S domains and the external circuit.

The elemental composition and phase purity were further verified using energy-dispersive X-ray spectroscopy (EDS) (Figure 4.5). The spectra exhibit distinct peaks for Cu and S, confirming the formation of Cu_2S, along with weaker signals of C and O originating from the rGO substrate. The measured atomic ratios (Cu ≈ 39.9%, S ≈ 28.4%, C ≈ 15.9%, O ≈ 15.8%) are consistent with the expected stoichiometry of copper sulfide integrated with oxygen-containing surface groups (–OH, C–O–C, C=O) that typically persist in reduced graphene oxide even after thermal reduction. The concurrent presence of Cu and S peaks without additional metallic or oxide signatures indicates that the embedded phase is compositionally pure and strongly anchored within the carbon framework. The residual oxygen also suggests partial yet beneficial reduction of GO, introducing defect sites and polar functionalities that facilitate Cu^{2+} coordination and enhance nanoparticle stabilization during synthesis.

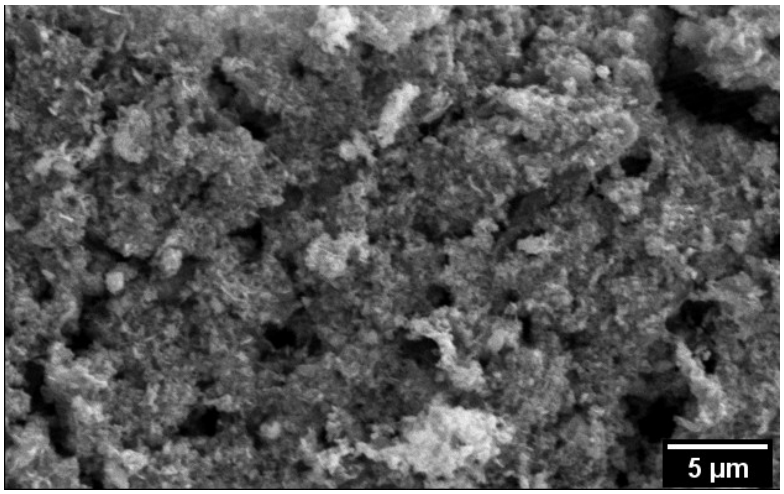

Figure 4.4 SEM images of the Cu_2S/rGO

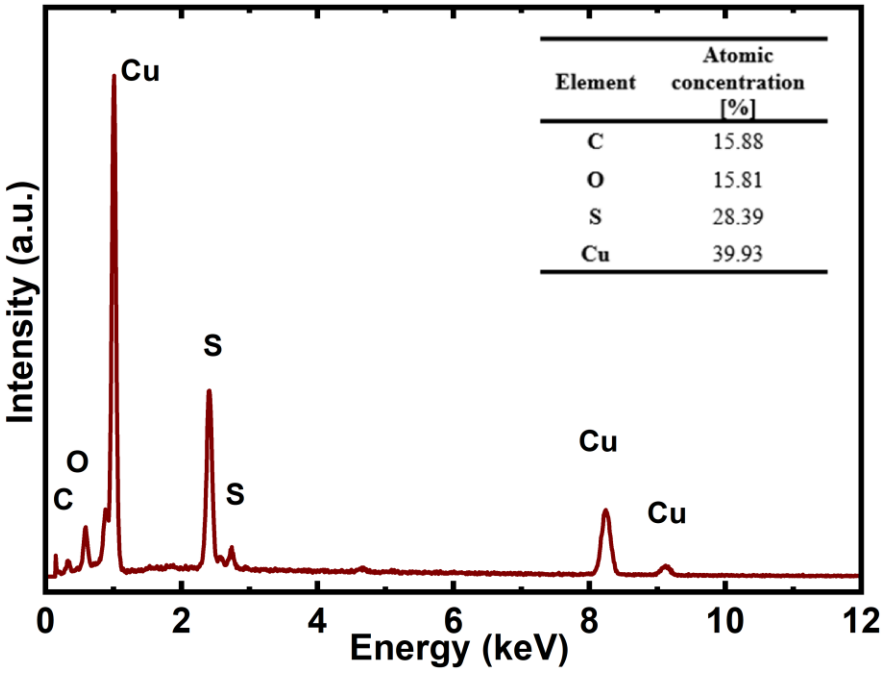

Figure 4.5 EDS spectra and atomic composition of the Cu_2S/rGO

Raman spectroscopy was employed to track the structural evolution of graphene oxide (GO) during its reduction to reduced graphene oxide (rGO). The pristine GO spectrum displays the characteristic D (~1350 cm^{-1}) and G (~1595 cm^{-1}) bands, where the relatively low ID/IG ratio indicates the presence of disrupted sp^2 carbon domains caused by oxygen-containing groups. When GO is mixed with glucose at a 1:1 mass ratio, a noticeable increase in the D-band intensity and a slight shift of the G band occur, implying partial restoration of the conjugated carbon framework due to mild reduction by glucose-derived intermediates. Following thermal annealing at 1000 °C for 5 h under an Ar atmosphere, the obtained rGO exhibits a more pronounced D band along with a distinct 2D feature around ~2700 cm^{-1}. The higher I_D/I_G ratio suggests the development of smaller yet more numerous sp^2 domains, consistent with the elimination of oxygen functionalities and structural rearrangement into turbostratic graphene layers. The appearance of the well-defined 2D band and the reduction of defect-related shoulders confirm significant graphitization and the

establishment of extended π–π conjugation, resulting in an electrically conductive rGO framework ideal for subsequent Cu_2S integration (Fig.4.6).

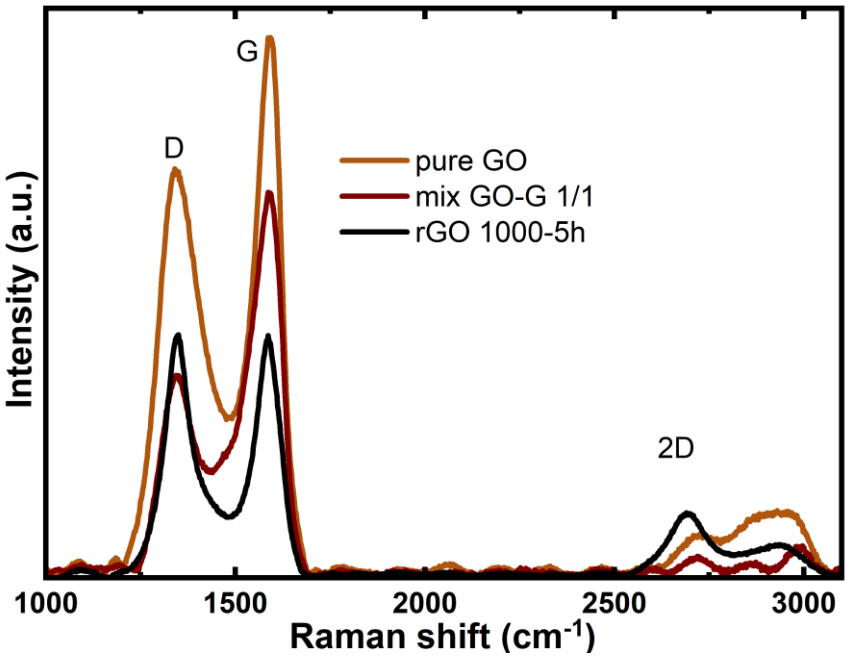

Figure 4.6 Raman Spectra of the GO and rGO

4.3.1.3 XPS

The surface chemical composition, elemental identification, and chemical environment of the samples were analyzed using X-ray photoelectron spectroscopy (XPS), as shown in Fig.4.7a. The high-resolution Cu $2p_{3/2}$ spectra of the three samples revealed distinct features. For CuS, a peak at 932.2 eV was observed and is attributed to the Cu^{2+} oxidation state, consistent with literature reports. In the case of Cu_2S, a peak at 932.4 eV was detected, corresponding to Cu^{+}, indicating a predominantly Cu(I) state in this sample. The Cu_2S/CuS composite exhibited two peaks at 932.4 and 932.7 eV, which are attributed to Cu^{+} in Cu_2S and Cu_2O, respectively. The presence of Cu_2O suggests that Cu_2S in the composite is susceptible to oxidation when exposed to

ambient conditions. The high-resolution S 2p spectra for CuS, Cu_2S, and Cu_2S/CuS are presented in Fig.4.7b. For CuS, the characteristic sulfur spin-orbit doublets S $2p_{3/2}$ and S $2p_{1/2}$ appeared at 162.1 and 163.0 eV, respectively, corresponding to the S^{2-} oxidation state. In the Cu_2S sample, these peaks were shifted to lower binding energies at 161.4 and 162.5 eV. This shift is attributed to differences in the sulfur chemical environment. Specifically, the lower binding energy in Cu_2S suggests a more metallic character due to stronger Cu–Cu interactions and fewer covalent S–S bonds. In contrast, CuS, with its greater covalent character and reduced metallic bonding, exhibits slightly higher binding energy values, implying increased electron density around sulfur atoms. For the Cu_2S/CuS composite, the sulfur doublet was observed at 161.8 and 162.8 eV, also corresponding to S^{2-}. These values fall between those of the individual CuS and Cu_2S samples, further confirming the composite nature and the influence of copper stoichiometry on the sulfur environment. The elemental composition derived from XPS analysis is summarized in Table 4.2. For CuS, a Cu/S molar ratio of 0.79 was recorded, whereas Cu_2S exhibited a higher ratio of 1.56, consistent with the EDS results and the expected copper enrichment in this phase. The Cu_2S/CuS composite showed a Cu/S ratio of 1.64, slightly higher than that of pure Cu_2S. This increase is attributed to partial oxidation of Cu_2S to Cu_2O, as evidenced in the Cu 2p spectra (Fig.4.7a). Signals for carbon and oxygen are primarily ascribed to the carbon tape used during analysis. Additionally, the presence of nitrogen in CuS and Cu_2S/CuS is linked to the use of the capping agent polyvinylpyrrolidone (PVP, C_6H_9NO) during synthesis (Krylova and Andrulevičius, 2009; Kundu and Chakraborty, 2024; Li et al., 2022; Xie et al., 2021; Yiming Zhang et al.).

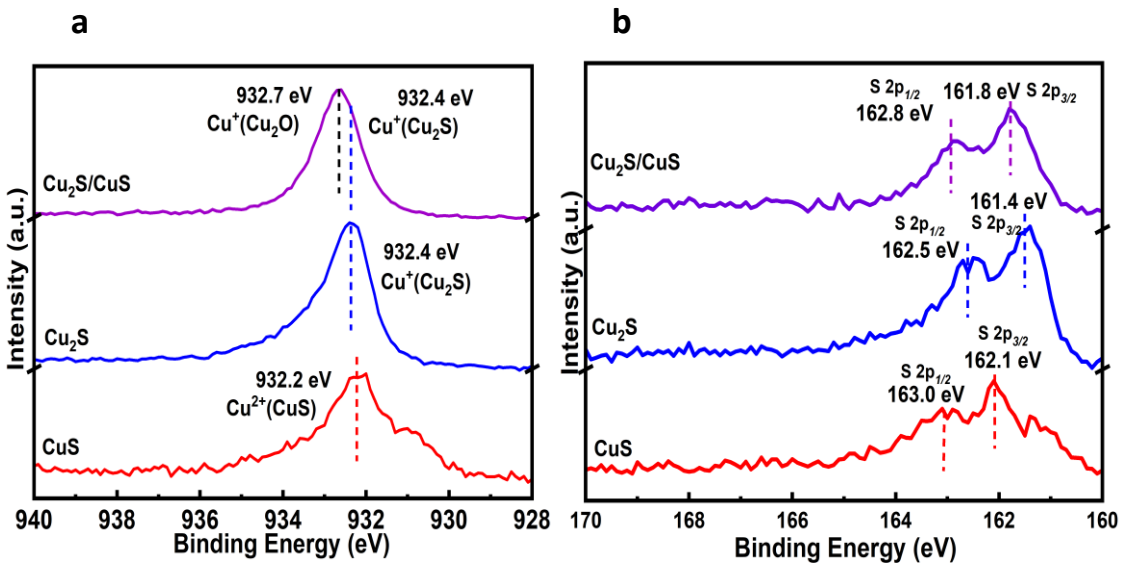

Figure 4.7. XPS spectra of CuS, Cu_2S, Cu_2S/CuS. a) HR-XPS spectra of Cu $2p_{3/2}$, b) HR-XPS spectra of S 2p

Table 4.2 Atomic composition of the CuS, Cu_2S, Cu_2S/CuS quantified by XPS survey

Element	Atomic composition (%)		
	CuS	Cu_2S	Cu_2S/CuS
S	13.31	18.62	9.92
Cu	10.58	29.09	16.28
C	52.05	41.78	51.46
N	10.35	-	9.45
O	13.72	10.52	12.89

4.3.2 Photocatalytic Performance

4.3.2.1 Effect of Photocatalyst Composition on PFOA and PFOS Degradation

The composition of Cu-based photocatalysts had a significant impact on the degradation of PFOA and PFOS. For PFOA, the $Cu_2S3/2$ catalyst initially exhibited the highest removal efficiency of 60%, indicating strong early-stage reactivity. However, over prolonged irradiation, Cu_2S surpassed $Cu_2S3/2$, achieving a higher degradation efficiency of approximately 66%, highlighting its superior long-term stability. The Cu_2S/rGO composite displayed the lowest activity, with only about 40% PFOA degradation, suggesting that the incorporation of reduced graphene oxide into the Cu_2S structure did not enhance but rather hindered photocatalytic performance. Regarding PFOS degradation, both $Cu_2S3/2$ and Cu_2S showed excellent activity, each achieving nearly 95% removal, demonstrating that both catalysts are highly effective for PFOS breakdown. In contrast, Cu_2S/rGO reached only around 76% degradation, again indicating a negative effect of reduced graphene oxide incorporation on photocatalytic efficiency. These results collectively suggest that while $Cu_2S3/2$ offers strong initial reactivity for PFOA, Cu_2S provides better long-term efficiency, and both Cu_2S and $Cu_2S3/2$ are highly effective for PFOS removal. Overall, the findings underscore the crucial role of catalyst composition in determining both the initial activity and sustained photocatalytic performance, and they justify focusing on simpler Cu_2S-based photocatalysts for subsequent optimization studies (Fig.4.8).

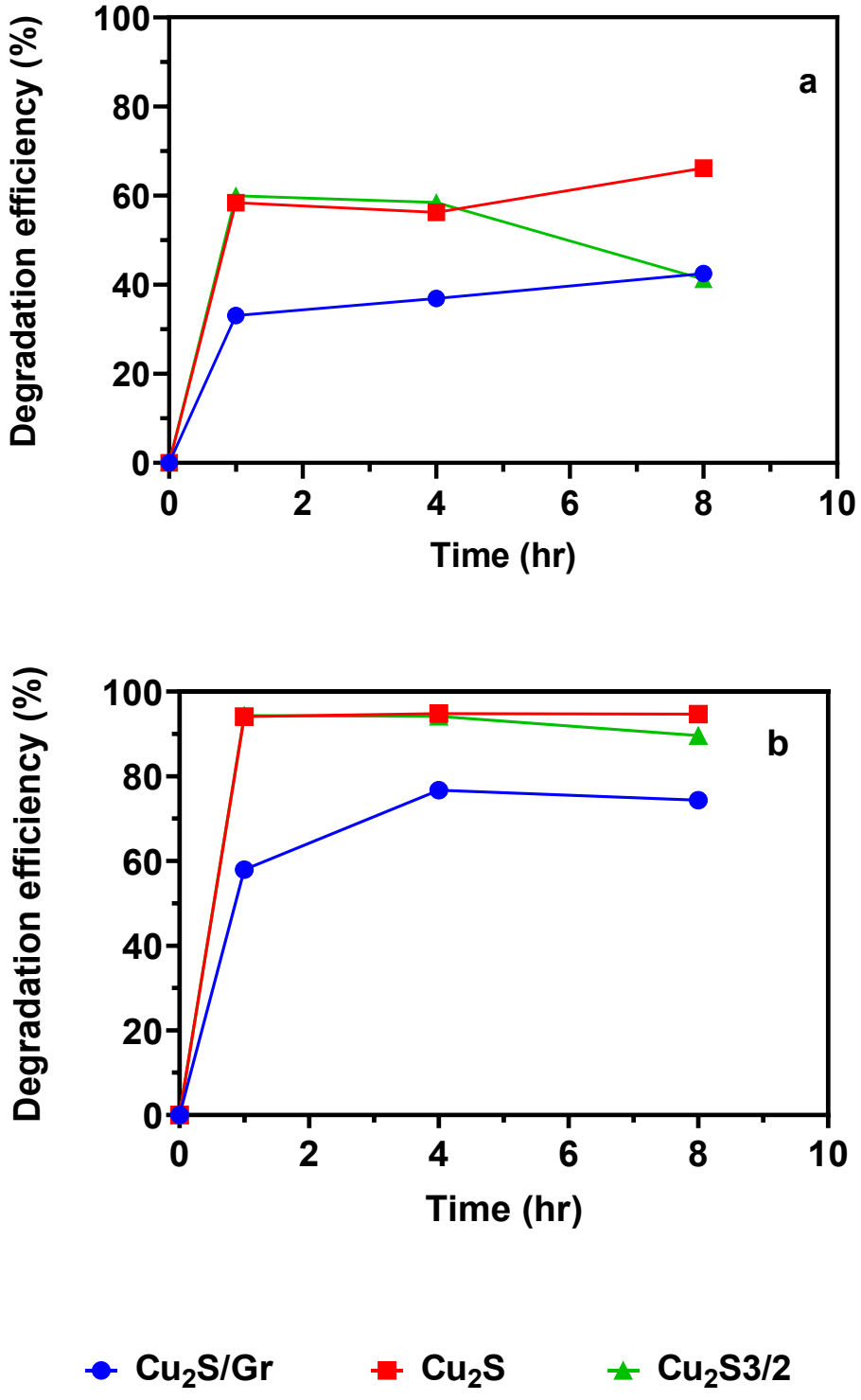

Figure 4.8 Degradation efficiency comparison of 1 mg/L solution between Cu_2S, Cu_2S/Gr, $Cu_2S3/2$ photocatalysts, without pH adjustment (pH = 4-5), 20 mg photocatalyst and 25 °C: a) PFOA b) PFOS

4.3.2.2 Pseudo-First-Order Kinetics and Pseudo-Second-Order Kinetics

The photocatalytic degradation of PFAS over the tested catalysts was evaluated using both pseudo-first-order and pseudo-second-order kinetic models, providing complementary insights into reaction dynamics and surface interactions. Under pseudo-first-order kinetics (Eq. 2), $Cu_2S3/2$ exhibited the highest rate constant (K), indicating a more efficient photodegradation pathway compared to Cu_2S and Cu_2S/rGO. This elevated K value reflects accelerated generation of reactive species, such as hydroxyl radicals (·OH), superoxide radicals ($O_2\cdot^-$), or photogenerated holes, and more effective utilization of incident photons, collectively enhancing PFAS breakdown under identical conditions. The superior performance of $Cu_2S3/2$ can be attributed to its p-type semiconducting nature and mixed-phase composition, which likely introduces defect sites, internal heterojunctions, or domain interfaces that facilitate charge separation, prolong carrier lifetimes, and suppress electron-hole recombination (Sayed et al., 2025). Such mechanisms are consistent with observations in copper-based sulfide photocatalysts, where internal electric fields arising from phase heterogeneity promote electron migration and reactive species formation (Qiao et al., 2023; Xu et al., 2025). Heterojunction analogues, including $Cu_2S/CdIn_2S_4$ Z-schemes and Cu_2S/CdS p–n junctions, illustrate that spatial separation of electrons and holes enhances redox activity and photocatalytic efficiency (Chen et al., 2015; Zhang et al., 2024). In contrast, Cu_2S/rGO displayed diminished activity, highlighting that reduced graphene oxide incorporation does not inherently improve performance; poor interfacial contact or mismatched energy levels can create recombination centers and reduce charge separation efficiency (Yuan et al., 2018). Complementary pseudo-second-order kinetics (Eq. 3) further elucidated the role of surface properties and catalyst composition in PFAS degradation. Here, a higher K value corresponds to stronger interactions between the catalyst surface and PFAS molecules, reflecting enhanced

adsorption or active site accessibility. $Cu_2S3/2$ again exhibited the highest rate constant, confirming that its unique composition and surface structure optimize interactions with PFAS, facilitating faster degradation. Conversely, Cu_2S/rGO displayed the lowest pseudo-second-order rate, likely due to poor synergy between Cu_2S and reduced graphene oxide or limited accessibility of active sites. Together, these kinetic analyses demonstrate that both structural heterogeneity, internal electric fields, and surface characteristics, including the Cu/S ratio, are critical determinants of photocatalytic efficiency. The combined insights from first- and second-order kinetics suggest that $Cu_2S3/2$'s superior performance arises from optimized charge dynamics, efficient photon absorption, and favorable surface interactions. Further experimental validation, such as reactive species trapping, time-resolved photoluminescence, or electron paramagnetic resonance spectroscopy, would provide direct evidence linking kinetic behavior to underlying photocatalytic mechanisms (Fernandes et al., 2024; Qiao et al., 2023) (Table 4.3).

$$\ln (C_t) = \ln (C_0) - k_1 t \quad (2)$$

$$1/C_t = (1/C_0) + k_2 t \quad (3)$$

Table 4.3. Comparison of Pseudo-First-Order Kinetics and Pseudo-Second-Order Kinetics for PFOA and PFOS among different photocatalysts

Photocatalyst	Pseudo-First-Order Kinetics K (min^{-1})		Pseudo-Second-Order Kinetics K (min^{-1})	
	PFOA	PFOS	PFOA	PFOS
Cu_2S/rGO	-0.475	-1.410	2E-06	1E-05
Cu_2S	-0.951	-3.376	6E-06	9E-05
Cu_2S 3/2	-0.989	-3.413	7E-06	9E-05

4.3.2.3. $Cu_2S3/2$ Photocatalyst Optimizations

PFOA degradation reached a maximum at 600 ppb and decreased at both lower (200 ppb) and higher (1 mg/L) initial concentrations (Fig. 4.9a), indicating a delicate balance between adsorption saturation, photon availability, and active site utilization. At low concentration (200 ppb), insufficient PFAS molecules may limit occupancy of active sites, reducing the rate of photocatalytic transformation. At high concentration (1 mg/L), surface sites on $Cu_2S3/2$ could become saturated, and PFAS molecules in solution may attenuate incident light, lowering the effective photon flux at catalytic centers (Fernandes et al., 2024).

Adsorption contributed approximately 16 % for PFOA and 28 % for PFOS (Fig. 4.9a,b), highlighting its important role in overall removal. Carbonaceous materials are known to concentrate PFAS near reactive surfaces, enhancing degradation efficiency when combined with photochemistry (Dey et al., 2024). The “concentrate and destroy” approach explains how preconcentration via adsorption followed by photocatalytic reaction improves performance.

PFOS exhibited consistently high removal efficiencies (95–99 %) across all tested concentrations (Fig. 4.9b). This suggests that $Cu_2S3/2$ provides both strong adsorption affinity and robust catalytic

turnover for sulfonic PFAS. Strong adsorption ensures rapid capture even at low concentrations, while efficient regeneration of active sites maintains high degradation at elevated PFOS levels (Zhang et al., 2021).

Overall, optimal removal at 600 ppb likely reflects the best combination of sufficient PFAS to occupy surface sites without significant light attenuation and strong adsorption to concentrate PFAS near active sites. Future mechanistic studies, such as reactive species trapping, photon flux measurements, and surface characterization before and after reaction, could clarify the contributions of adsorption and photocatalysis and guide the design of photocatalysts for environmentally relevant PFAS concentrations (Fig. 4.10).

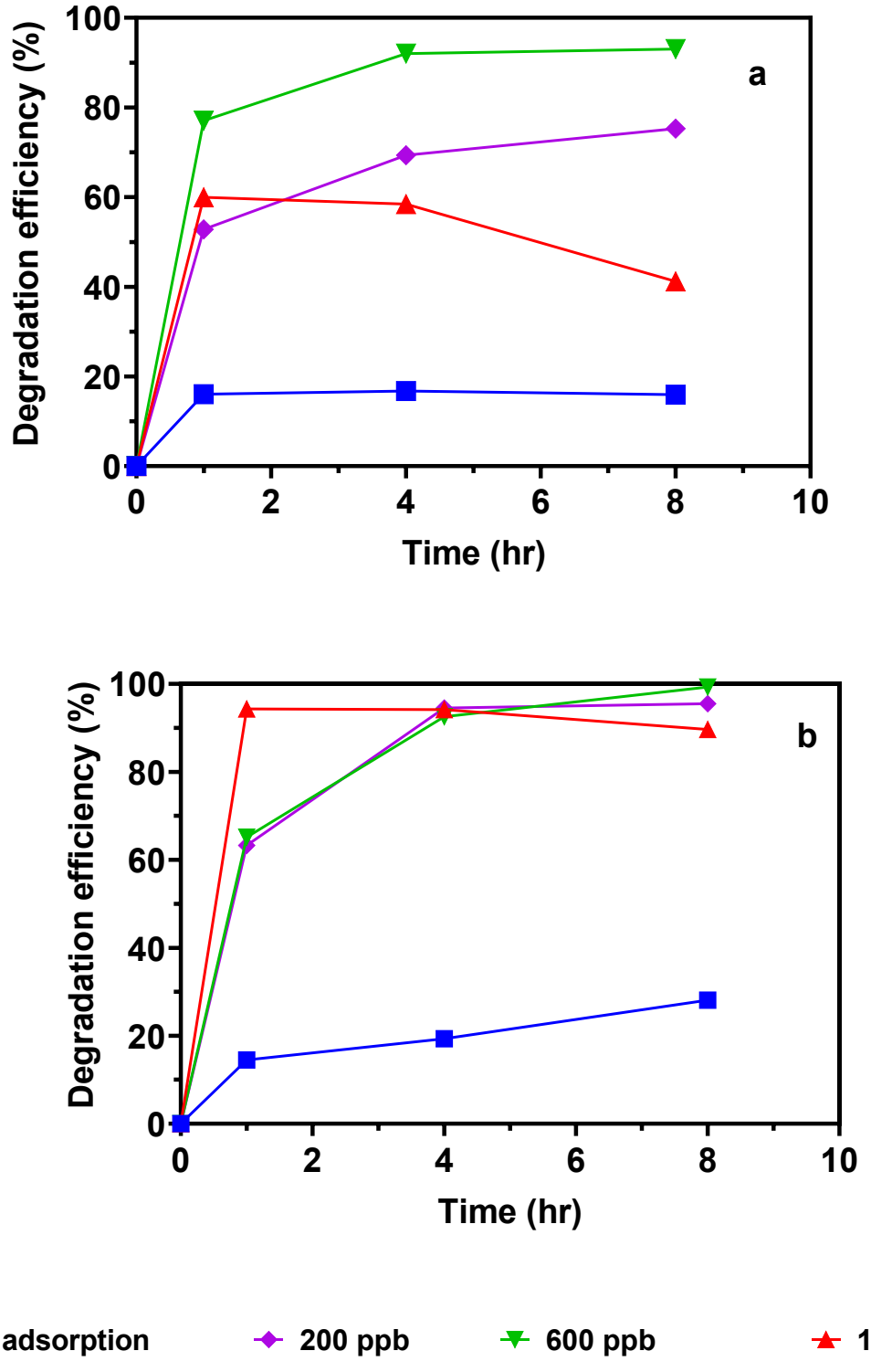

Figure 4.9 Degradation efficiency comparison in different solution concentrations with $Cu_2S3/2$ photocatalyst (20mg), without pH adjustment (pH = 4-5), and 2 °C: a) PFOA b) PFOS

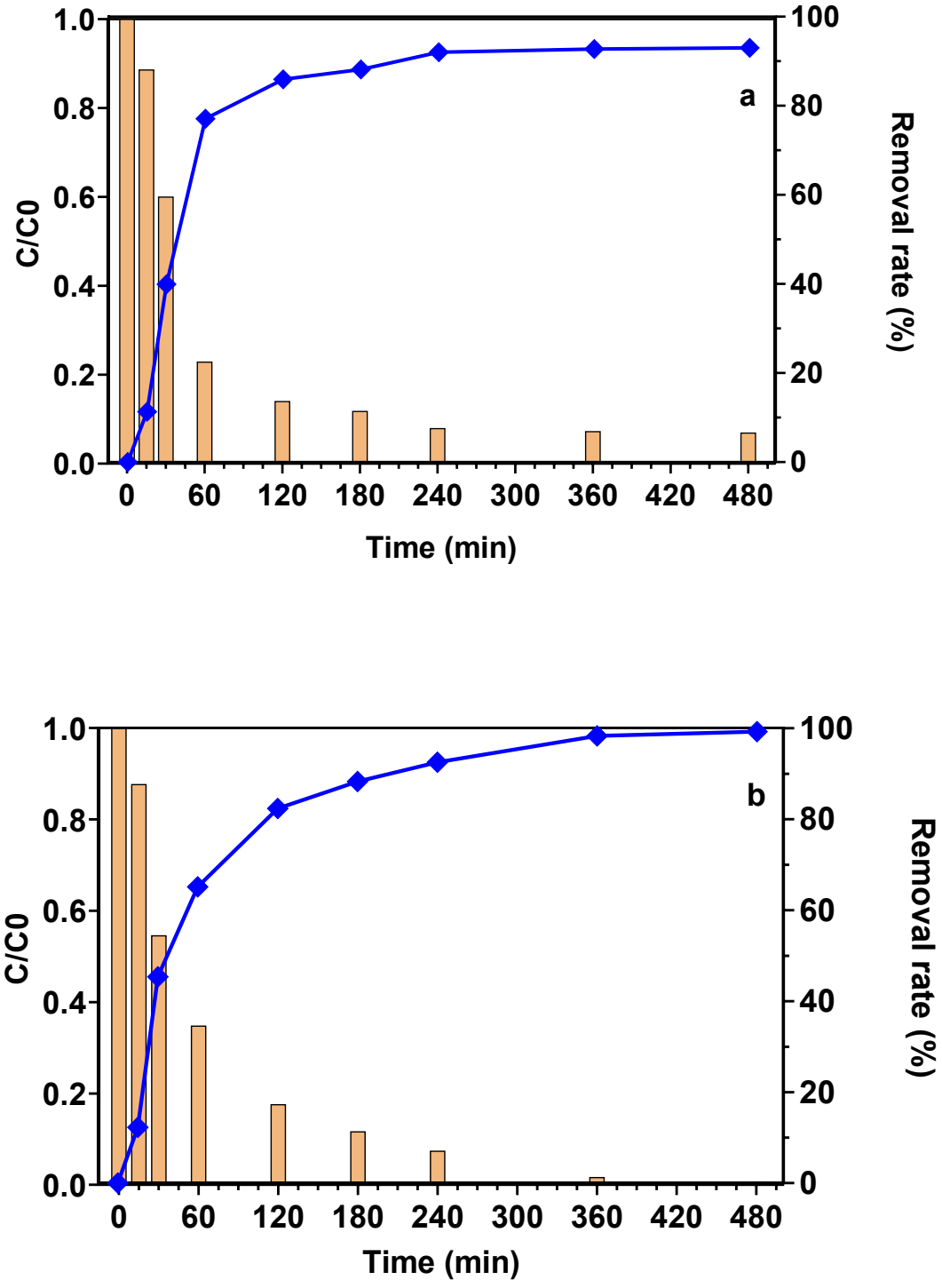

Figure 4.10 Removal efficiency for 600 ppb solution with $Cu_2S3/2$ photocatalyst (20mg), without pH adjustment (pH = 4-5) and 25°C: a) PFOA, b) PFOS

The adsorption performance of the photocatalysts was evaluated prior to the photocatalytic experiments and the results are presented in Figure 4.11. The catalysts exhibited relatively low adsorption capacities, as indicated by only a small decrease in C/C_0 over the 480 minute dark adsorption period. An initial rapid adsorption occurred within the first 30 minutes, after which the removal rates stabilized, suggesting that surface active sites were quickly occupied (Dey et al., 2024). Beyond this period, negligible further adsorption was observed, indicating limited interactions between PFAS molecules and catalyst surfaces.

These findings demonstrate that adsorption contributes minimally to overall PFAS removal under the tested conditions. Consequently, the subsequent degradation under light irradiation can be attributed primarily to photocatalytic activity rather than physical adsorption (Ricardo J.C. Fernandes, 2025). This observation is consistent with previous studies showing that Cu_2S-based photocatalysts exhibit low inherent adsorption capacity for PFAS and rely on photogenerated reactive species to achieve efficient degradation (Zhang et al., 2021).

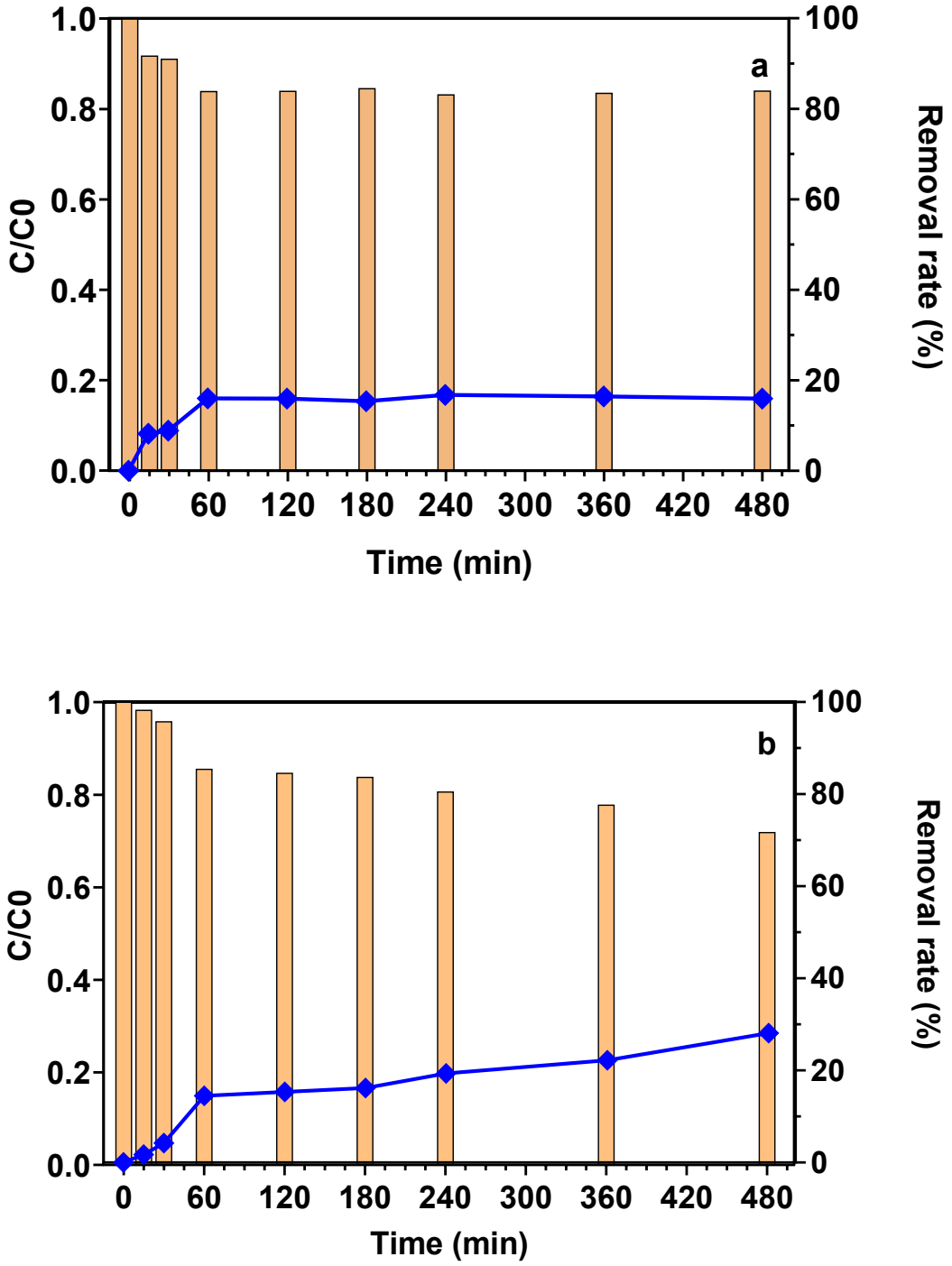

Figure 4.11 Adsorption test for 1 mg/L solution with $Cu_2S3/2$ photocatalyst (20mg), without pH adjustment (pH = 4-5) and 25°C: a) PFOA b) PFOS

The influence of catalyst dosage on PFAS degradation was investigated by comparing 20 mg and 10 mg loadings of $Cu_2S_3/_2$, with the results presented in Figure 4.12. Reducing the catalyst to 10 mg caused a pronounced decrease in removal efficiency for both PFOA and PFOS. For PFOA, degradation remained minimal over the 480 minute reaction period, with C/C_0 values close to 1 and removal rates limited to approximately 20 %. PFOS removal was similarly suppressed, reaching only 15 to 18 % under the lower catalyst loading.

This pronounced decline in activity can be explained by the reduced number of available active sites coupled with a diminished generation of reactive species under UV irradiation. The limited availability of surface sites restricts PFAS adsorption and the subsequent production of hydroxyl and superoxide radicals, thereby constraining photocatalytic conversion. These observations underscore the critical importance of optimizing catalyst dosage to ensure sufficient active sites and efficient photon utilization, which are essential for achieving effective PFAS degradation under environmentally relevant concentrations (Dey et al., 2024; Ricardo J.C. Fernandes, 2025).

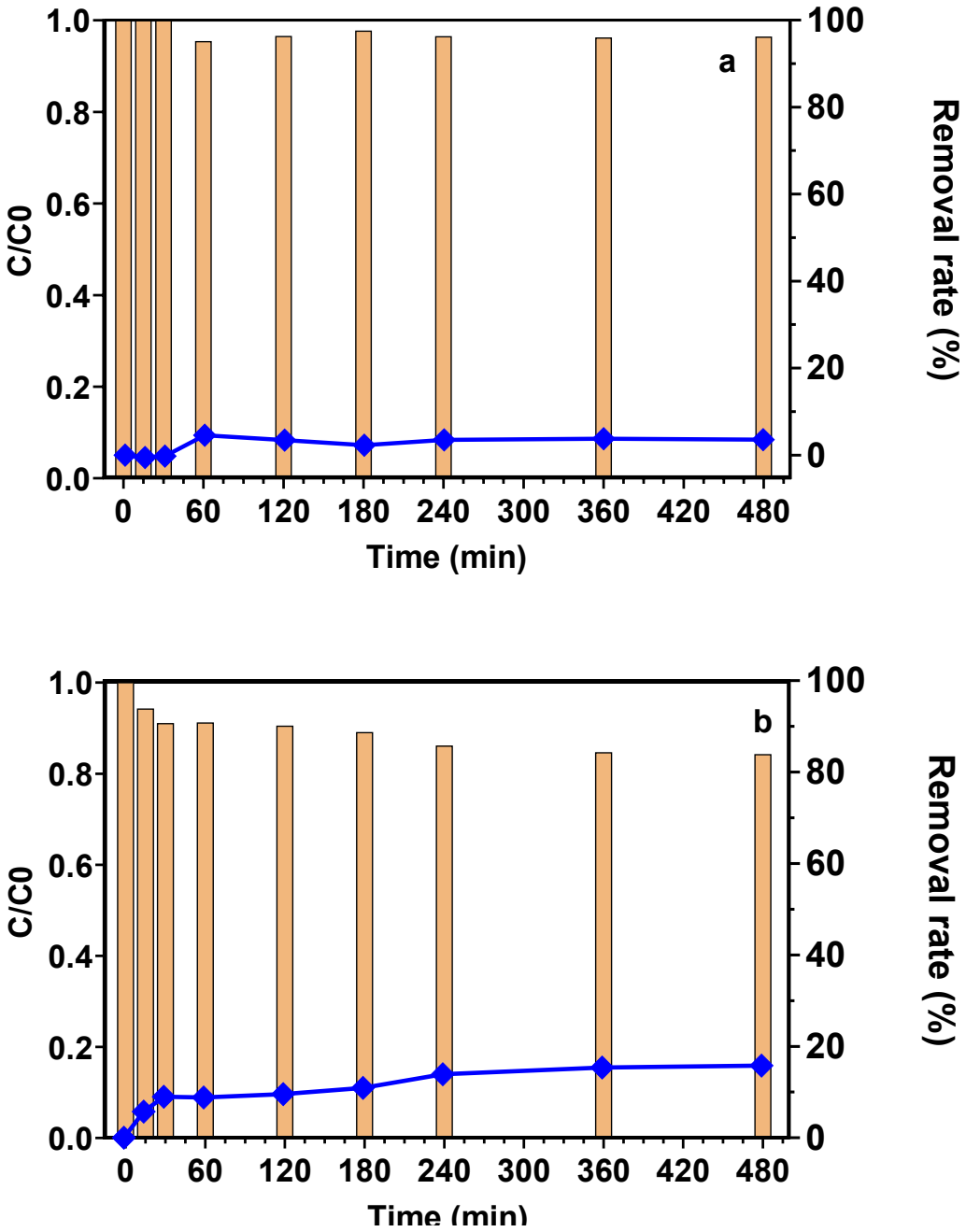

Figure 4.12 Removal efficiency for 1 mg/L solution with $Cu_2S3/2$ photocatalyst (10 mg) without pH adjustment (pH = 4-5) and 25°C: a) PFOA, b) PFOS

Figure 4.13 shows the removal performance of 20 mg $Cu_2S3/2$ during its second cycle in a 1 mg/L solution of PFOA and PFOS at 25 °C without pH adjustment (pH 4–5). A dramatic decrease in PFOA removal was observed: whereas ~60 % was removed in the first cycle, only about 15–20 % was eliminated over 480 minutes in the second cycle. PFOS removal followed a similar trend, dropping from 94 % in the first cycle to approximately 25–30 % in the second.

This pronounced decline suggests that the catalyst surface becomes deactivated or fouled after initial use. One plausible explanation is the strong binding of PFAS species, which could block or poison active sites and inhibit the formation of reactive intermediates. Such behavior is consistent with observations in metal ion-exchanged zeolite systems, where repeated photodegradation leads to attenuated performance due to site saturation and structural rearrangements (Qian et al., 2024). These findings highlight a fundamental challenge in maintaining the reusability of $Cu_2S3/2$ in PFAS treatment and underscore the need for regeneration strategies or alternative catalyst designs to preserve long-term activity.

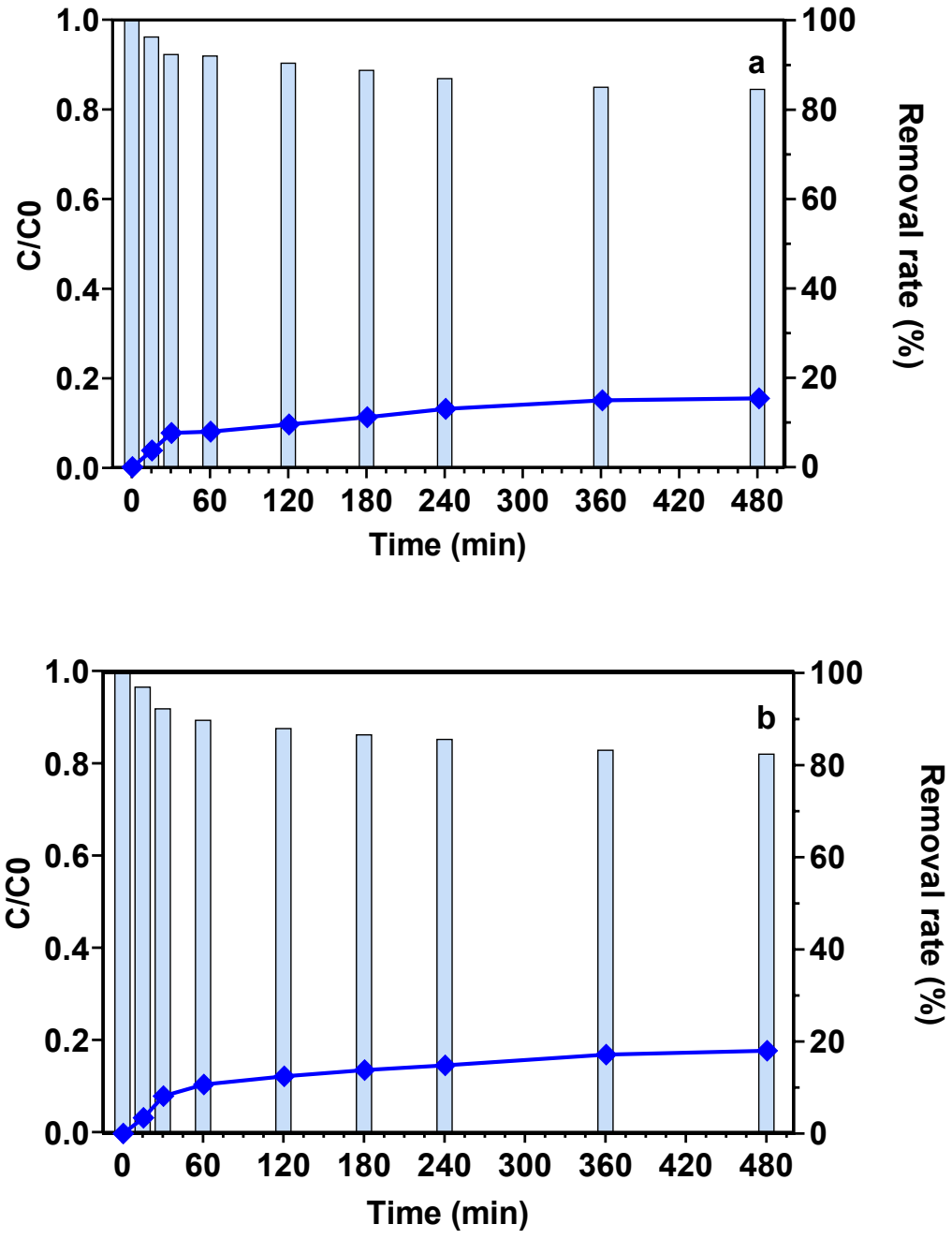

Figure 4.13 Second cycle $Cu_2S3/2$ reuse 1 mg/L solution, without pH adjustment (pH = 4-5), 20 mg photocatalyst and 25°C: a) PFOA b) PFOS

4.4. Conclusion

Copper sulfide-based nanomaterials demonstrate exceptional photocatalytic activity for the degradation of persistent PFAS pollutants, including PFOA and PFOS. Among the synthesized catalysts, mixed-phase $Cu_2S3/2$ achieved the highest performance, with nearly complete removal of PFOS (99 %) and substantial degradation of PFOA (93 %), while phase-pure Cu_2S also exhibited strong activity. In contrast, the Cu_2S/rGO composite displayed only moderate efficiency, indicating that the incorporation of reduced graphene oxide alone does not significantly enhance photocatalytic performance in this system.

These results emphasize the critical importance of phase composition and structural characteristics in determining photocatalytic efficiency. The superior performance of $Cu_2S3/2$ illustrates that optimized copper sulfide phases can effectively generate reactive species and facilitate pollutant mineralization. Overall, the study establishes Cu_2S-based nanomaterials as highly promising candidates for the efficient removal of PFAS from aqueous environments, providing a compelling foundation for the development of practical water treatment technologies.

Chapter 5: General Discussion and Conclusions

Per- and polyfluoroalkyl substances (PFAS), particularly PFOA and PFOS, pose a critical global challenge due to their extreme persistence, bioaccumulative properties, and adverse health and ecological impacts. Conventional treatment technologies such as adsorption, ion exchange, and membrane can achieve partial removal of PFAS from water matrices; however, they are fundamentally constrained, as they primarily separate or concentrate contaminants rather than promote their chemical destruction. Moreover, these approaches are often associated with high operational costs, secondary waste generation, and limited effectiveness toward short-chain PFAS, highlighting the urgent need for innovative, sustainable, and scalable remediation strategies. Advanced oxidation processes (AOPs), particularly photocatalysis, have gained increasing attention because they offer the potential for direct C–F bond cleavage, defluorination, and mineralization of PFAS under relatively mild conditions. Nevertheless, the effectiveness of photocatalytic systems remains highly dependent on catalyst properties, including band-gap energy, charge-carrier separation efficiency, surface reactivity, and structural stability during operation.

In this context, copper sulfide–based photocatalysts, notably Cu_2S and its mixed phases, present several attractive attributes, including tunable electronic structures, strong absorption in the visible to near-infrared region, and the capacity to form heterojunctions that suppress charge recombination. In the present study, CuS, Cu_2S, $Cu_2S3/2$, and a Cu_2S/rGO composite were systematically synthesized, characterized, and evaluated for their photocatalytic performance in degrading PFOA and PFOS under UV irradiation. Among the investigated materials, $Cu_2S3/2$ exhibited the highest activity, achieving near-complete degradation of PFOS (99 %) and

substantial degradation of PFOA (93 %), while Cu_2S showed comparably high performance, and Cu_2S/rGO demonstrated moderate enhancement. These results indicate that phase composition, interfacial charge transfer, and surface–pollutant interactions play decisive roles in determining PFAS degradation efficiency. The findings also underscore the potential benefits of nanostructuring and integration with conductive carbonaceous supports, although further optimization is required to fully exploit synergistic effects.

The implications of this work extend beyond proof-of-concept laboratory demonstrations. The successful degradation of PFAS using copper-based nanomaterials provides a promising framework for developing low-cost and environmentally benign photocatalysts for water treatment applications. Nonetheless, several limitations warrant careful consideration. First, photocatalytic experiments were conducted under idealized conditions, including UV irradiation, controlled pH, and single-contaminant systems, which do not fully represent the complexity of real wastewater matrices where coexisting ions, natural organic matter, and fluctuating physicochemical conditions may suppress performance. Second, the long-term stability, recyclability, and potential copper ion leaching from the catalysts must be systematically evaluated to ensure environmental safety and practical viability. Third, although high degradation efficiencies were observed, the underlying reaction pathways, key intermediates, and extent of complete mineralization remain insufficiently resolved. Future studies should therefore incorporate advanced analytical techniques to identify transformation products, quantify released fluoride, and elucidate the roles of reactive oxygen species and charge carriers in PFAS defluorination.

Looking forward, further research should prioritize extending the applicability of Cu_2S-based photocatalysts to solar or simulated solar irradiation, given the limited contribution of UV light in natural sunlight. Approaches such as semiconductor coupling, elemental doping, and hierarchical

nanostructure design may substantially enhance light utilization and catalytic efficiency. In addition, transitioning from batch systems to continuous-flow reactors and pilot-scale studies will be essential to assess real-world feasibility. Evaluating catalyst performance against a broader range of PFAS, including short-chain and emerging alternatives, will also be critical for establishing comprehensive treatment potential.

In conclusion, this study advances PFAS remediation research by demonstrating the high photocatalytic efficiency of copper-based nanomaterials, particularly $Cu_2S3/2$, for the degradation of PFOA and PFOS in aqueous systems. By addressing intrinsic limitations of conventional treatment technologies, these findings contribute to the development of next-generation, cost-effective, and environmentally sustainable remediation strategies. Although further optimization, mechanistic clarification, and validation under realistic conditions are required, this work establishes Cu_2S-based photocatalysts as strong candidates for future large-scale PFAS treatment, supporting ongoing efforts to protect water resources and public health from persistent emerging contaminants.

References

Aditi P, AHM A, Debra R, Ni-Bin C, Ramesh G. Per and poly-fluoroalkyl substances (PFAS) as a contaminant of emerging concern in surface water: A transboundary review of their occurrences and toxicity effects. J. Hazard. Mater. 2021; 419: 126361.

Ahmed MB, Alam MM, Zhou JL, Xu B, Johir MAH, Karmakar AK, et al. Advanced treatment technologies efficacies and mechanism of per-and poly-fluoroalkyl substances removal from water. J. Process Saf. Environ. Prot. 2020; 136: 1-14.

Ahmed SN, Haider W. Heterogeneous photocatalysis and its potential applications in water and wastewater treatment: a review. Nanotechnology 2018; 29: 342001.

Ain NU, Nasir JA, Khan Z, Butler I, Rehman Z. Copper sulfide nanostructures: synthesis and biological applications. RSC Advances 2022; 12: 7550-7567.

Ait-Karra A, Zakir O, Mourak A, Elouakassi N, Almaggoussi A, Idouhli R, et al. Elaboration of CuS nanomaterials via hydrothermal route: Examining physical properties and photocatalytic potential. Journal of Physics and Chemistry of Solids 2023.

Aswathy P, Gandhimathi R, Ramesh S, Nidheesh PJS, Technology P. Removal of organics from bilge water by batch electrocoagulation process. 2016; 159: 108-115.

Ateia M, Maroli A, Tharayil N, Karanfil T. The overlooked short- and ultrashort-chain poly- and perfluorinated substances: A review. Chemosphere 2019; 220: 866-882.

Banayan Esfahani E, Mohseni M. Fluence-based photo-reductive decomposition of PFAS using vacuum UV (VUV) irradiation: Effects of key parameters and decomposition mechanism. J. Environ. Chem. Eng. 2022; 10.

Bentuo Xu MBA, John L. Zhou a, Ali Altaee, Minghong Wu, Gang Xu. Photocatalytic removal of perfluoroalkyl substances from water and wastewater: Mechanism, kinetics and controlling factors. Chemosphere 2017; 189: 717-729.

Bouteh E, Bentel MJ, Cates EL. Semiconductor-hydrophobic material interfaces as a new active site paradigm for photocatalytic degradation of perfluorocarboxylic acids. J. Hazard. Mater. 2023; 453: 131437.

Brent L, Marco P, Salma A, Daria B, Viviane Y. Application of photocatalytic ozonation with a WO_3/TiO_2 catalyst for PFAS removal under UVA/visible light. Sci. Total Environ. 2022; 843: 157006.

Brown JB, Conder JM, Arblaster JA, Higgins CP. Assessing Human Health Risks from Per- and Polyfluoroalkyl Substance (PFAS)-Impacted Vegetable Consumption: A Tiered Modeling Approach. Environmental Science & Technology 2020; 54: 15202-15214.

Cao C-S, Wang J, Yang L, Wang J, Zhang Y, Zhu L. A review on the advancement in photocatalytic degradation of poly/perfluoroalkyl substances in water: Insights into the mechanisms and structure-function relationship. The Science of the total environment 2024: 174137.

Cardoso I, Da Silva LP, Da Silva JE. Nanomaterial-Based Advanced Oxidation/Reduction Processes for the Degradation of PFAS. Nanomaterials 2023a; 13.

Chang P, Wang Y, Wang Y, Zhu Y. Current Trends on In_2o_3 Based Heterojunction Photocatalytic Systems In Photocatalytic Application. SSRN Electron. J.

2022.

Chen J, Wang S, Wang S, Tang R, Chen H. Facilely prepared Bi_4O_7 modified commercial Ga_2O_3 with optimized photocatalytic efficiency for perfluorooctanoic acid degradation. J. Appl. Surf. Sci. 2024; 673: 160877.

Chen X, Yuan T, Yang X, Ding S, Ma M. Insights into Photo/Electrocatalysts for the Degradation of Per- and Polyfluoroalkyl Substances (PFAS) by Advanced Oxidation Processes. Catalysts 2023; 13: 1308.

Chen Y, Qin Z, Wang X, Guo X, Guo L. Noble-metal-free Cu_2S-modified photocatalysts for enhanced photocatalytic hydrogen production by forming nanoscale p–n junction structure. RSC Advances 2015; 5: 18159-18166.

Chowdhury N, Choi H. Photocatalytic degradation of perfluorooctanoic acid on Pb-doped TiO_2 coated with reduced graphene oxide. Water Environ. Res. 2023; 95: e10871.

Dai C, Sheng Z, Tian X, Nie Y. Chalcogen Elements in Regulating the Local Electron Density of Cu_2X for an Efficient Heterogeneous Fenton-like Process. ACS Appl Mater Interfaces 2023; 15: 11324-11332.

Deng F, Peng J, Li X, Luo X, Ganguly P, Pillai SC, et al. Metal sulfide-based Z-scheme heterojunctions in photocatalytic removal of contaminants, H_2 evolution and CO_2 reduction: Current status and future perspectives. J. Clean. Prod. 2023.

Dey D, Shafi T, Chowdhury S, Dubey BK, Sen R. Progress and perspectives on carbon-based materials for adsorptive removal and photocatalytic degradation of perfluoroalkyl and polyfluoroalkyl substances (PFAS). Chemosphere 2024; 351: 141164.

Duan L, Wang B, Heck K, Guo S, Clark CA, Arredondo J, et al. Efficient Photocatalytic PFOA Degradation over Boron Nitride. Environ. Sci. Technol. Lett. 2020; 7: 613-619.

Ehsan BE, M M. Fluence-based photo-reductive decomposition of PFAS using vacuum UV (VUV) irradiation: Effects of key parameters and decomposition mechanism. J. Environ. Chem. Eng. 2022; 10.

Fernandes R, Silva A, Cardoso B, Coutinho PJG, Pereira L. Potential of Photocatalytic Nanomaterials for PFOA and PFOS degradation: Challenges and Opportunities. Journal of Environmental Chemical Engineering 2024.

Fu C, Xu X, Zheng C, Liu X, Zhao D, Qiu W. Photocatalysis of aqueous PFOA by common catalysts of In_2O_3, Ga_2O_3, TiO_2, CeO_2 and CdS: influence factors and mechanistic insights. Environ. Geochem. Health 2022; 44: 2943-2953.

Ge J, Zhang Y, Heo Y-J, Park S-J. Advanced Design and Synthesis of Composite Photocatalysts for the Remediation of Wastewater: A Review. Catalysts 2019; 9: 122.

Gomez-Ruiz B, Ribao P, Diban N, Rivero MJ, Ortiz I, Urtiaga A. Photocatalytic degradation and mineralization of perfluorooctanoic acid (PFOA) using a composite TiO_2 -rGO catalyst. J. Hazard. Mater. 2018; 344: 950-957.

Grandjean P, Clapp R. Perfluorinated Alkyl Substances: Emerging Insights Into Health Risks. J. New Solut. 2015; 25: 147-63.

Guo M, Zhao T, Xing Z, Qiu Y, Pan K, Li Z, et al. Hollow Octahedral Cu2-xS/CdS/Bi2S3 p-n-p Type Tandem Heterojunctions for Efficient Photothermal Effect and Robust Visible-Light-Driven Photocatalytic Performance. ACS applied materials & interfaces 2020.

Guo Q, Zhou C, Ma Z, Yang X. Fundamentals of TiO_2 Photocatalysis: Concepts, Mechanisms, and Challenges. Adv. Mater. 2019; 31: e1901997.

Habib A, Khan MS, Zubair M, Hasan IU. Ni-Doped In(2)O(3) Nanoparticles and Their Composite with rGO for Efficient Degradation of Organic Pollutants in Wastewater under Visible Light Irradiation. Int J Mol Sci 2023; 24.

Haghighi P, Alijani S, Bazyari A, Thompson LT. Visible light dye degradation over fluorinated mesoporous $TiO_2 - WO_3 - Bi_2O_3/SiO_2$ nanocomposite photocatalyst-adsorbent using immersion well reactor. J. Photochem. Photobiol. A Chem. 2022; 426.

He H, Sun M, Wu D, Di G, Fei X. Cu(III) generation and air sparging extend catalytic effectiveness of Cu2S/H2O2 from neutral to acidic condition: performance and mechanism in comparison with CuS/H2O2. Journal of Cleaner Production 2021; 278.

Humayun M, Wang C, Luo W. Recent Progress in the Synthesis and Applications of Composite Photocatalysts: A Critical Review. Small Methods 2022; 6: e2101395.

Huu-Tuan Do L-APT, Ngoc Han Dao Nguyen,, Chao-Wei Huang QVLaV-HN. Tailoring photocatalysts and elucidating mechanisms of photocatalytic degradation of perfluorocarboxylic acids (PFCAs) in water: a comparative overview. J. Chem. Technol. Biotechnol. 2020; 95: 2569-2578.

Hwang E-B, Park Y, Kim J, Paik T, Ha DH. Facile Sulfurization under Ambient Condition with Na2S to Fabricate Nanostructured Copper Sulfide. Nanomaterials 2021; 11.

Jain RB. Association between thyroid profile and perfluoroalkyl acids: data from NHNAES 2007-2008. Environ. Res. 2013; 126: 51-9.

Jean Noel Uwayezu IC, Patrick van Hees, Patrik Karlsson, Jurate Kumpiene. Validation of UV/persulfate as a PFAS treatment of industrial wastewater and environmental samples. J. Water Process Eng. 2023.

Jing Li X-YC, Ru-Bai Lei, Jin-Feng Lai, Tong-Mei Ma, Yang Li Highly thermally conductive graphene film produced using glucose under low-temperature thermal annealing. 2019.

Junker AL, Christensen FMS, Bai L, Jorgensen MK, Fojan P, Khalil A, et al. Emerging investigator series: Photocatalytic Treatment of PFAS in a Single-step Ultrafiltration Membrane Reactor. J. Environ. Sci. Water Res. Technol. 2024.

Juve JA, Donoso Reece JA, Wong MS, Wei Z, Ateia M. Photocatalysts for chemical-free PFOA degradation - What we know and where we go from here? J. Hazard. Mater. 2024; 462: 132651.

Khan MF, Paul Guin J, Thampi RK, Sullivan JA, Murphy CD. Enhanced removal of perfluorooctanoic acid with sequential photocatalysis and fungal treatment. Environ. Sci. Pollut. Res. Int. 2023; 30: 91478-91486.

Kociołek-Balawejder E, Gibas A, Baszczuk A, Jasiorski M, Jacukowicz-Sobala I. Transformation of CuO and Cu2O particles into CuxS within the polymeric matrix of anion exchangers, and its structural and morphological implications. Reactive and Functional Polymers 2023.

Kotthoff M, Müller J, Jürling H, Schlummer M, Fiedler D. Perfluoroalkyl and polyfluoroalkyl substances in consumer products. Environ. Sci. Pollut. Res. Int. 2015; 22: 14546-59.

Krylova V, Andrulevičius M. Optical, XPS and XRD Studies of Semiconducting Copper Sulfide Layers on a Polyamide Film. 2009; 2009: 304308.

Kundu A, Chakraborty B. Surface Structure to Tailor the Electrochemical Behavior of Mixed-Valence Copper Sulfides during Water Electrolysis. JACS Au 2024; 4: 642-656.

Leung SCE, Shukla P, Chen D, Eftekhari E, An H, Zare F, et al. Emerging technologies for PFOS/PFOA degradation and removal: A review. Sci. Total Environ. 2022; 827: 153669.

Li F, Wei Z, He K, Blaney L, Cheng X, Xu T, et al. A concentrate-and-destroy technique for degradation of perfluorooctanoic acid in water using a new adsorptive photocatalyst. Water Res. 2020; 185: 116219.

Li X, Zhang P, Jin L, Shao T, Li Z, Cao J. Efficient photocatalytic decomposition of perfluorooctanoic acid by indium oxide and its mechanism. Environ Sci Technol 2012; 46: 5528-34.

Li Z, Zhang P, Shao T, Wang J, Jin L, Li X. Different nanostructured In_2O_3 for photocatalytic decomposition of perfluorooctanoic acid (PFOA). J Hazard Mater 2013; 260: 40-6.

Li ZH, Egbo KO, Lv XH, Wang Y, Yu KM, Liu CP. Electronic structure and properties of Cu2-xS thin films: Dependence of phase structures and free-hole concentrations. Applied Surface Science 2022; 572.

Liang J, Guo L, Xiang B, Wang X, Tang J, Liu Y. Research Updates on the Mechanism and Influencing Factors of the Photocatalytic Degradation of Perfluorooctanoic Acid (PFOA) in Water Environments. Molecules 2023; 28.

Liu C, Zhu X, You L, Gin KY, Chen H, Chen B. Per/polyfluoroalkyl substances modulate plasmid transfer of antibiotic resistance genes: A balance between oxidative stress and energy support. Water Res. 2023; 240: 120086.

Liu F, Guan X, Xiao F. Photodegradation of per-and polyfluoroalkyl substances in water: A review of fundamentals and applications. J. Hazard. Mater. 2022a; 439: 129580.

Liu J, Mejia Avendaño S. Microbial degradation of polyfluoroalkyl chemicals in the environment: a review. J. Environ. Int. 2013; 61: 98-114.

Liu X, Duan X, Bao T, Hao D, Chen Z, Wei W, et al. High-performance photocatalytic decomposition of PFOA by BiOX/TiO_2 heterojunctions: Self-induced inner electric fields and band alignment. J. Hazard. Mater. 2022b; 430: 128195.

Liu X, Wei W, Xu J, Wang D, Song L, Ni BJ. Photochemical decomposition of perfluorochemicals in contaminated water. Water Res 2020; 186: 116311.

Liu Y, Liu M, Yin D, Qiao L, Fu Z, Swihart M. Selective Cation Incorporation into Copper Sulfide Based Nanoheterostructures. ACS nano 2018; 12 8: 7803-7811.

Liu Z, Chen Z, Gao J, Yu Y, Men Y, Gu C, et al. Accelerated Degradation of Perfluorosulfonates and Perfluorocarboxylates by UV/Sulfite + Iodide: Reaction Mechanisms and System Efficiencies. Environ. Sci. Technol. 2022c; 56: 3699-3709.

Luo J, Li W, Yin R, Liu Q, Xin X, Yang L, et al. Photocatalyst degradation of perfluorooctanoic acid in water: Mechanisms, approaches, and perspectives. J. Sep. Purif. Technol. 2024a: 126503.

Luo P, Zhang Y, Peng Z, He Q, Zhao W, Zhang W, et al. Photocatalytic degradation of perfluorooctanoic acid (PFOA) from water: A mini review. Environ. Pollut. 2024b; 343: 123212.

Lv X, Cao L, Fu Y, Guo J, Yang J, Huang Y, et al. Morphology-Controlled Synthesis of Cu_2S for Efficient Oxygen Evolution Reaction. Journal of Electroanalytical Chemistry 2022.

Ma L, Ai X, Chen Y, Liu P, Lin C, Lu K, et al. Improved Photocatalytic Activity via n-Type ZnO/p-Type NiO Heterojunctions. Nanomaterials (Basel) 2022; 12.

Mahpishanian S, Zhou MC, Foudazi R. Magnetic amino-functionalized graphene oxide nanocomposite for PFAS removal from water. Environ. Sci. Adv. 2024; 3.

Mastropietro T, Bruno R, Pardo E, Armentano D. Reverse osmosis and nanofiltration membranes for highly efficient PFASs removal: overview, challenges and future perspectives. Dalton Trans. 2021; 50 16: 5398-5410.

McCleaf P, Englund S, Östlund Å, Lindegren K, Wiberg K, Ahrens L. Removal efficiency of multiple poly- and perfluoroalkyl substances (PFASs) in drinking water using granular activated carbon (GAC) and anion exchange (AE) column tests. Water Res. 2017; 120: 77-87.

Mills A, Davies RH, Worsley D. Water purification by semiconductor photocatalysis. J. Chem. Soc. Rev. 1993; 22: 417-425.

Nawaz F, Ali M, Ahmad S, Yong Y, Rahman S, Naseem M, et al. Carbon based nanocomposites, surface functionalization as a promising material for VOCs (volatile organic compounds) treatment. Chemosphere 2024; 364: 143014.

Neuwald IJ, Hübner D, Wiegand HL, Valkov V, Borchers U, Nödler K, et al. Ultra-Short-Chain PFASs in the Sources of German Drinking Water: Prevalent, Overlooked, Difficult to Remove, and Unregulated. Environ. Sci. Technol. 2022; 56: 6380-6390.

Nikam A, Pandey A, Fernandes G, Kulkarni S, Mutalik S, Padya B, et al. Copper sulphide based heterogeneous nanoplatforms for multimodal therapy and imaging of cancer: Recent advances and toxicological perspectives. Coordination Chemistry Reviews 2020; 419: 213356.

Olatunde OC, Kuvarega AT, Onwudiwe DC. Photo enhanced degradation of polyfluoroalkyl and perfluoroalkyl substances. Heliyon 2020; 6: e05614.

Park K, Ali I, Kim JO. Photodegradation of perfluorooctanoic acid by graphene oxide-deposited TiO_2 nanotube arrays in aqueous phase. J Environ Manage 2018; 218: 333-339.

Pelaez M, Nolan NT, Pillai SC, Seery MK, Falaras P, Kontos AG, et al. A review on the visible light active titanium dioxide photocatalysts for environmental applications. J. Appl. Catal. B Environ. 2012; 125: 331-349.

Podder A, Sadmani A, Reinhart D, Chang N, Goel R. Per and poly-fluoroalkyl substances (PFAS) as a contaminant of emerging concern in surface water: A transboundary review of their occurrences and toxicity effects. J. Hazard. Mater. 2021; 419: 126361.

Post GB, Cohn PD, Cooper KR. Perfluorooctanoic acid (PFOA), an emerging drinking water contaminant: a critical review of recent literature. Environ Res. 2012; 116: 93-117.

Poulopoulos SG, Yerkinova A, Ulykbanova G, Inglezakis VJ. Photocatalytic treatment of organic pollutants in a synthetic wastewater using UV light and combinations of TiO_2, H_2O_2 and Fe(III). PLoS One 2019; 14: e0216745.

Qanbarzadeh M, DiGiacomo L, Bouteh E, Alhamdan EZ, Mason MM, Wang B, et al. An Ultraviolet/Boron Nitride Photocatalytic Process Efficiently Degrades Poly-/Perfluoroalkyl Substances in Complex Water Matrices. Environ. Sci. Technol. Lett. 2023; 10: 705-710.

Qian L, Zhao H, Schierz A, Mackenzie K, Georgi A. A Deep Insight into Perfluorooctanoic Acid Photodegradation Using Metal Ion-Exchanged Zeolites. ACS ES&T Engineering 2024; 4: 748-757.

Qiao F, Qian S, Liu W, Zhou T, Yang J, Zhao J, et al. Cu_2O/Cu_2S microstructure regulation towards high efficiency photocatalytic hydrogen production and its theoretical mechanism analysis. Cryst. Eng. Comm. 2023; 25: 4939-4945.

Raaja Rajeshwari M, Kokilavani S, Sudheer Khan S. Recent developments in architecturing the g-C3N4 based nanostructured photocatalysts: Synthesis, modifications and applications in water treatment. Chemosphere 2022; 291: 132735.

Ramirez-Ubillus MA, Wang A, Zou S, Chumbimuni-Torres KY, Zhai L. Morphological Effect on the Surface Activity and Hydrogen Evolution Catalytic Performance of Cu_2O and Cu_2O/rGO Composites. 2023; 7: 403.

Ren Q, He Y, Wang H, Sun Y, Dong F. Photo-Switchable Oxygen Vacancy as the Dynamic Active Site in the Photocatalytic NO Oxidation Reaction. ACS Catalysis 2022; 12: 14015-14025.

Ricardo J.C. Fernandes ARS, Beatriz D. Cardoso, Paulo J.G. Coutinho, Luciana Pereira Potential of photocatalytic nanomaterials for PFOA and PFOS degradation: Challenges and opportunities. Journal of Environmental Chemical Engineering 2025.

Roy P, Srivastava S. Nanostructured copper sulfides: synthesis, properties and applications. CrystEngComm 2015; 17: 7801-7815.

Sadia M, Nollen I, Helmus R, Ter Laak TL, Béen F, Praetorius A, et al. Occurrence, Fate, and Related Health Risks of PFAS in Raw and Produced Drinking Water. Environ. Sci. Technol. 2023; 57: 3062-3074.

Sahu SP, Qanbarzadeh M, Ateia M, Torkzadeh H, Maroli AS, Cates EL. Rapid Degradation and Mineralization of Perfluorooctanoic Acid by a New Petitjeanite $Bi_3O(OH)(PO_4)_2$ Microparticle Ultraviolet Photocatalyst. Environ. Sci. Technol. Lett. 2018; 5: 533-538.

Sayed M, Qi K, Wu X, Zhang L, Garcia H, Yu J. Cu-based S-scheme photocatalysts. Chem. Soc. Rev. 2025; 54: 4874-4921.

Schneider J, Matsuoka M, Takeuchi M, Zhang J, Horiuchi Y, Anpo M, et al. Understanding TiO_2 photocatalysis: mechanisms and materials. Chem. Rev. 2014; 114: 9919-86.

Shao T, Zhang P, Jin L, Li Z. Photocatalytic decomposition of perfluorooctanoic acid in pure water and sewage water by nanostructured gallium oxide. J. Appl. Catal. B Environ. 2013; 142: 654-661.

Song Z, Dong X, Wang N, Zhu L, Luo Z, Fang J, et al. Efficient photocatalytic defluorination of perfluorooctanoic acid over BiOCl nanosheets via a hole direct oxidation mechanism. J. Chem. Eng. J. 2017; 317: 925-934.

Tabatabaei M, Cho DW, Fahad S, Jeong DW, Hwang JH. Photocatalytic innovations in PFAS removal: Emerging trends and advances. Sci Total Environ 2025; 980: 179567.

Tang L, Li A, Kong M, Dionysiou DD, Duan X. Effects of wavelength on the treatment of contaminants of emerging concern by UV-assisted homogeneous advanced oxidation/reduction processes. Sci. Total Environ. 2023; 899: 165625.

Trojanowicz M, Bojanowska-Czajka A, Bartosiewicz I, Kulisa K. Advanced Oxidation/Reduction Processes treatment for aqueous perfluorooctanoate (PFOA) and perfluorooctanesulfonate (PFOS) – A review of recent advances. Chem. Eng. J. 2018; 336: 170-199.

USEPA. National Primary Drinking Water Regulations, 2024.

Verma S, Mezgebe B, Hejase CA, Sahle-Demessie E, Nadagouda MN. Photodegradation and photocatalysis of per- and polyfluoroalkyl substances (PFAS): A review of recent progress. Next Mater. 2024; 2: 1-12.

Verma S, Varma RS, Nadagouda MN. Remediation and mineralization processes for per- and polyfluoroalkyl substances (PFAS) in water: A review. Sci. Total Environ. 2021; 794: 148987.

Wang H, Zhang L, Chen Z, Hu J, Li S, Wang Z, et al. Semiconductor heterojunction photocatalysts: design, construction, and photocatalytic performances. Chem. Soc. Rev. 2014; 43: 5234-44.

Wang S, Riedinger A, Li H, Fu C, Liu H, Li L, et al. Plasmonic copper sulfide nanocrystals exhibiting near-infrared photothermal and photodynamic therapeutic effects. ACS nano 2015; 9 2: 1788-1800.

Wang Y, Liu M, Wu C, Gao J, Li M, Xing Z, et al. Hollow Nanoboxes Cu2-x S@ZnIn2 S4 Core-Shell S-Scheme Heterojunction with Broad-Spectrum Response and Enhanced Photothermal-Photocatalytic Performance. Small 2022.

Wanninayake DM. Comparison of currently available PFAS remediation technologies in water: A review. J. Environ. Manage. 2021a; 283: 111977.

Wen J, Li H, Ottosen LDM, Lundqvist J, Vergeynst L. Comparison of the photocatalytic degradability of PFOA, PFOS and GenX using Fe-zeolite in water. Chemosphere 2023a; 344: 140344.

Wen Y, AK, GSD, HL, MFS, Yang Y, et al. Photocatalytic degradation of perfluorooctanoic acid by a temperature transformed metal-organic framework MIL-177-HT. SSRN Electron. J. 2023b.

Wu X, Qin N, Yan L, Ji R, Wu D, Hou Z, et al. In situ preparation of a $Bi_2O_2CO_3$/BiOI with 2D/2D p-n heterojunction photocatalyst for water purification under visible light. Front Chem 2022; 10: 1102528.

Xia C, Lim X, Yang H, Goodson BM, Liu J. Degradation of per-and polyfluoroalkyl substances (PFAS) in wastewater effluents by photocatalysis for water reuse. J. Water Process Eng. 2022; 46: 102556.

Xie N, Ma D-D, Wu Y-L, Wu X-T, Zhu Q-L. Hierarchical Cu2S hollow nanowire arrays for highly efficient hydrogen evolution reaction. Sustainable Energy & Fuels 2021; 5: 2633-2639.

Xin X, Kim J, Ashley DC, Huang CH. Degradation and Defluorination of Per- and Polyfluoroalkyl Substances by Direct Photolysis at 222 nm. J. ACS ES. T. Water 2023; 3: 2776-2785.

Xu B, Ahmed M, Zhou J, Altaee A, Wu M, Xu G. Photocatalytic removal of perfluoroalkyl substances from water and wastewater: Mechanism, kinetics and controlling factors. Chemosphere 2017; 189: 717-729.

Xu B, Liu S, Zhou JL, Zheng C, Weifeng J, Chen B, et al. PFAS and their substitutes in groundwater: Occurrence, transformation and remediation. J. Hazard. Mater. 2021; 412: 125159.

Xu B, Zhou JL, Altaee A, Ahmed MB, Johir MAH, Ren J, et al. Improved photocatalysis of perfluorooctanoic acid in water and wastewater by Ga_2O_3/UV system assisted by peroxymonosulfate. J. Chemosphere 2020; 239: 124722.

Xu R, Arif M, Pan G, Xu L, Zhu T. Designed formation of Cu_2S hierarchical nanostructures as self-supported photoelectrodes for photo-supercapacitors. Nanoscale Adv. 2025; 7: 5058-5066.

Xu W, Zhu S, Liang Y, Li Z, Cui Z, Yang X-J, et al. Nanoporous CuS with excellent photocatalytic property. Scientific Reports 2015; 5.

Yang H, Park S-J, Lee C-G. Enhanced removal of perfluoroalkyl substances using MMO-TiO_2 visible light photocatalyst. Alex. Eng. J. 2024; 87: 31-38.

Yao X, Zuo J, Wang YJ, Song NN, Li HH, Qiu K. Enhanced Photocatalytic Degradation of Perfluorooctanoic Acid by Mesoporous Sb_2O_3/TiO_2 Heterojunctions. Front. Chem. 2021; 9: 690520.

Yaoyao Wu YL, Chihhsiang Fang, Prof. Chuanhao Li. Highly Efficient Degradation of Perfluorooctanoic Acid over a MnOx-Modified Oxygen-Vacancy-Rich In_2O_3 Photocatalyst. ChemCatChem 2019; 11: 2297-2303.

Yashir N, Sun Q, Zhang X, Ma M, Wang D, Feng Y, et al. Co-occurrence of microplastics, PFASs, antibiotics, and antibiotic resistance genes in groundwater and their composite impacts on indigenous microbial communities: A field study. Sci. Total Environ. 2025; 961: 178373.

Yiming Zhang, Xiaoyan Yang, Yonglin Wang, Peng Zhang DL, Yongwei Li, Zhouzheng Jin, et al. Insight into l-cysteine-assisted growth of Cu2S nanoparticles on exfoliated MoS2 nanosheets for effective photoreduction removal of Cr(VI).

Yin P, Hu Z, Song X, Liu J, Lin N. Activated Persulfate Oxidation of Perfluorooctanoic Acid (PFOA) in Groundwater under Acidic Conditions. Int. J. Environ. Res. Public Health 2016; 13.

Yin S, Villagrán D. Design of nanomaterials for the removal of per- and poly-fluoroalkyl substances (PFAS) in water: Strategies, mechanisms, challenges, and opportunities. Sci. Total Environ. 2022; 831: 154939.

Yuan B, Gao Q, Zhang X, Duan L, Chen L, Mao Z, et al. Reduced graphene oxide (RGO)/Cu_2S composite as catalytic counter electrode for quantum dot-sensitized solar cells. Electrochimica Acta 2018; 277: 50-58.

Zango ZU, Khoo KS, Garba A, Kadir HA, Usman F, Zango MU, et al. A review on superior advanced oxidation and photocatalytic degradation techniques for perfluorooctanoic acid (PFOA) elimination from wastewater. Environ. Res. 2023; 221: 115326.

Zareitalabad P, Siemens J, Hamer M, Amelung W. Perfluorooctanoic acid (PFOA) and perfluorooctanesulfonic acid (PFOS) in surface waters, sediments, soils and wastewater - A review on concentrations and distribution coefficients. Chemosphere 2013; 91: 725-32.

Zelekew OA, Wang Z, Gu Y, Wu Y-N. Recent Progress on Photoactive Heterogeneous Photocatalysts for the Degradation of Per-and Polyfluoroalkyl Substances (PFAS): Mechanisms, DFT Calculations, Limitations, and Future Prospects. Journal of Environmental Chemical Engineering 2024.

Zhang D, Luo Q, Gao B, Chiang SY, Woodward D, Huang Q. Sorption of perfluorooctanoic acid, perfluorooctane sulfonate and perfluoroheptanoic acid on granular activated carbon. Chemosphere 2016a; 144: 2336-42.

Zhang L, Ran J, Qiao SZ, Jaroniec M. Characterization of semiconductor photocatalysts. Chem. Soc. Rev. 2019a; 48: 5184-5206.

Zhang S, Sun J, Ju H. Z-Scheme Heterojunction of Hierarchical $Cu_2S/CdIn_2S_4$ Hollow Cubes to Boost Photoelectrochemical Performance. Small 2024; 20: e2405712.

Zhang W, Zhang D, Liang Y. Nanotechnology in remediation of water contaminated by poly- and perfluoroalkyl substances: A review. Environ. Pollut. 2019b; 247: 266-276.

Zhang X, Lohmann R, Dassuncao C, Hu XC, Weber AK, Vecitis CD, et al. Source Attribution of Poly- and Perfluoroalkyl Substances (PFASs) in Surface Waters from Rhode Island and the New York Metropolitan Area. Environ. Sci. Technol. Lett. 2016b; 3: 316-321.

Zhang Y, Yang X, Wang Y, Zhang P, Liu D, Li Y, et al. Insight into l-cysteine-assisted growth of Cu_2S nanoparticles on exfoliated MoS_2 nanosheets for effective photoreduction removal of Cr(VI). Applied Surface Science 2020; 518.

Zhang YL, Wang WL, Lee MY, Yang ZW, Wu QY, Huang N, et al. Promotive effects of vacuum-UV/UV (185/254 nm) light on elimination of recalcitrant trace organic contaminants by UV-AOPs during wastewater treatment and reclamation: A review. Sci. Total. Environ. 2022; 818: 151776.

Zhang Z, Sarkar D, Datta R, Deng Y. Adsorption of perfluorooctanoic acid (PFOA) and perfluorooctanesulfonic acid (PFOS) by aluminum-based drinking water treatment residuals. Journal of Hazardous Materials Letters 2021; 2.

Zhao D, Tang X, Liu P, Huang Q, Li T, Ju L. Recent Progress of Ion-Modified TiO_2 for Enhanced Photocatalytic Hydrogen Production. Molecules 2024; 29.

Zhu C, Xu J, Song S, Wang J, Li Y, Liu R, et al. TiO_2 quantum dots loaded sulfonated graphene aerogel for effective adsorption-photocatalysis of PFOA. Sci Total Environ 2020; 698: 134275.